1.24 Deep Earth Structure: Seismic Scattering in the Deep Earth

PM Shearer, University of California, San Diego, La Jolla, CA, USA

1.24.1 Introduction

Most seismic analyses of Earth structure rely on observations of the travel times and waveforms of direct seismic waves that travel along ray paths determined by Earth's large-scale velocity structure. These observations permit inversions for radially averaged P-wave and S-wave velocity profiles as well as three-dimensional (3D) perturbations. However, smaller-scale velocity or density perturbations cause some fraction of the seismic energy to be scattered in other directions, usually arriving following the main phase as incoherent energy over an extended time interval. This later-arriving wave train is termed the coda of the direct phase. Given the number of different scattering events and the complexity of the scattered wavefield, it is generally impossible to resolve individual scatterers. Instead, coda-wave observations are modeled using random media theories that predict the average energy in the scattered waves as a function of scattering angle, given the statistical properties of the velocity and density perturbations. In this way, it is possible to characterize Earth's heterogeneity at much smaller scales than can be imaged using tomography or other methods.

The fact that direct seismic waves can be observed in the Earth indicates that this scattering must be relatively weak so that a significant fraction of the seismic energy remains in the primary arrivals. In contrast, scattering on the Moon is proportionally much stronger than in the Earth, preventing the easy observation of direct P and S waves at global distances (at least at the recorded frequencies of the available data) and complicating inversions for lunar structure. In addition to facilitating observations of direct arrivals, weak (as opposed to strong) scattering also can simplify modeling by permitting use of single-scattering theory (i.e., the Born approximation). However, it is now clear that accurate modeling of scattering in the lithosphere, and possibly deeper in the mantle as well, requires calculations based on multiple-scattering theories. Fortunately, increased computer power makes these calculations computationally feasible.

Although both body waves and surface waves exhibit scattering, my emphasis in this chapter is on observations and modeling of deep-Earth scattering, for which body waves provide the primary constraints. In addition, I also will give more attention to the mantle and core than the lithosphere, which has been the focus of the majority of coda studies to date. Finally, I will only briefly summarize the different scattering theories. For more details on these topics, the reader should consult the book by Sato and Fehler (1998, 2012), which provides an extensive review of scattering theory and analysis methods, as well as a comprehensive summary of crustal and lithospheric studies.

1.24.2 Scattering Theory

Wave scattering from random heterogeneities is a common phenomenon in many fields of science, and theoretical modeling approaches have been extensively developed in physics, acoustics, and seismology. Solving this problem for the full elastic wave equation (i.e., for both P and S waves) in the presence of strong perturbations in the elastic tensor and density is quite difficult, so various simplifying approximations are often applied. These include assuming an isotropic elastic tensor, using first-order perturbation theory in the case of weak

 http://dx.doi.org/10.1016/B978-0-444-53802-4.00018-X

scattering, using the diffusion equation for very strong scattering, and assuming correlations among the velocity and density perturbations.

1.24.2.1 Single-Scattering Theory and Random Media

For sufficiently weak velocity and density perturbations, most scattered energy will have experienced only one scattering event and can be adequately modeled using single-scattering theory. The mathematics in this case is greatly simplified if we assume that the primary waves are unchanged by their passage through the scattering region (the Born approximation). The total energy in the seismic wavefield therefore increases by the amount contained in the scattered waves, and energy conservation is not obeyed. Thus, this approximation is only valid when the scattered waves are much weaker than the primary waves, which is the case in the Earth when the velocity and density perturbations are relatively small (quantifying exactly how small depends upon the frequency of the waves and the source–receiver distance). Single-scattering theory is sometimes called Chernov theory after Chernov (1960). Detailed descriptions of Born scattering theory for elastic waves are contained in Wu and Aki (1985a,b), Wu (1989), and Sato and Fehler (1998, 2012). A review of the properties (elasticity, conductivity, and permeability) and statistics of random heterogeneous materials is given in the text by Torquato (2002).

Single-scattering theory provides equations that give the average scattered power as a function of the incident and scattered wave types (i.e., P or S), the power of the incident wave, the local volume of the scattering region, the bulk and statistical properties of the random medium, the scattering angle (the angle between the incident wave and the scattered wave), and the seismic wave number ($k = 2n/A$, where A is the wavelength). A general random medium could have separate perturbations in P velocity, S velocity, and density, but in practice, a common simplification is to assume a linear scaling relationship among the perturbations (e.g., Sato, 1990) and/or to assume zero density perturbations. However, as pointed out by Hong et al. (2004), density variations can have an important influence on scattering properties. Performing the actual calculation for a specific source–receiver geometry involves integrating the contributions of small volume elements over the scattering region of interest. Each volume element will have a specific scattering angle and geometric spreading factors for the source–scatterer and scatterer–receiver ray paths.

The nature of the scattering strongly depends upon the relative length scales of the heterogeneity and the seismic waves. The scale of perturbations in a random medium can be characterized by the autocorrelation function (ACF), with the correlation distance, a, providing a rough measure of the average size of the 'blobs' in many commonly assumed forms for the ACF (e.g., Gaussian, exponential, and van Karman). Figure 1 shows examples of random realizations of the Gaussian and exponential ACF models. If the heterogeneity is large compared to the seismic wavelength ($a \gg \Lambda$, ka is large), then forward scattering predominates and becomes increasingly concentrated near the direction of the incident wave as ka increases. In the limit of large ka, the energy remains along the primary ray path and scattering effects do not need to be taken into account. Alternatively, if the blobs are small compared to the seismic wavelength ($a \ll \Lambda$, ka is small), then the scattering is often approximated as isotropic and the scattered power scales as k^4a^3. In the limit of small ka, the scattering strength goes to zero and the medium behaves like a homogeneous solid. As discussed by Aki and Richards (1980, pp. 749–750), scattering effects are strongest when a and A are of comparable size (i.e., when $ka \sim 2\pi$).

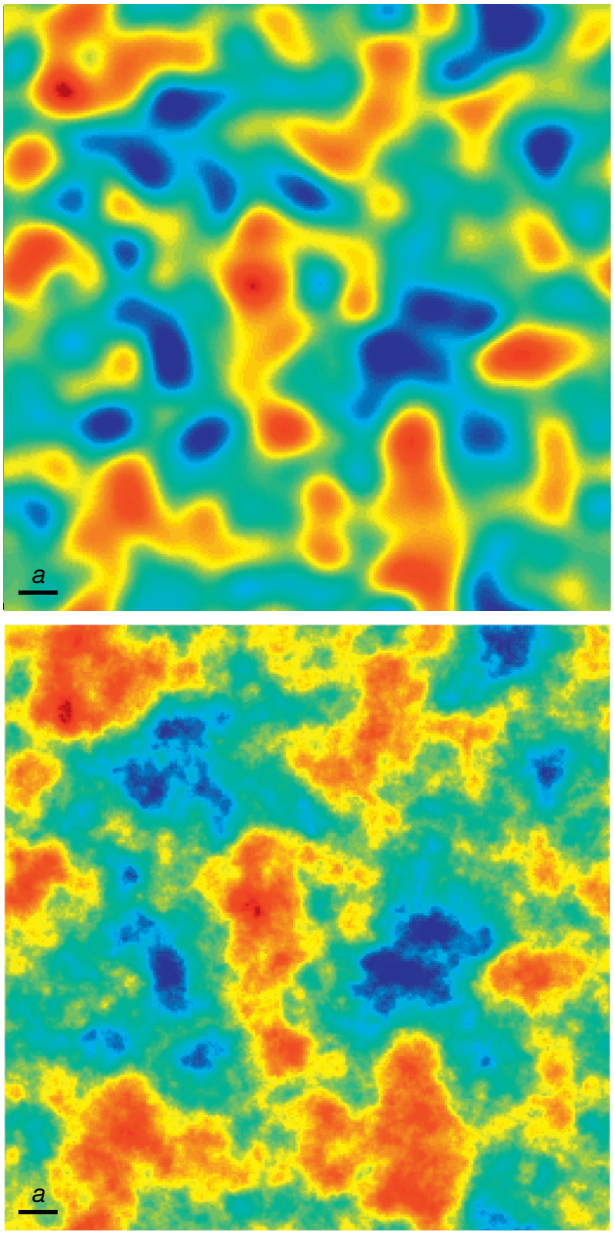

Figure 1 Examples of random media defined by a Gaussian autocorrelation function (top) and an exponential autocorrelation function (bottom). The correlation distance, a, is indicated in the lower left corner. The exponential medium has more structure at short wavelengths than the Gaussian medium.

Aki and Chouet (1975) presented an important application of single-scattering theory to predict coda decay rates for local earthquakes. For a colocated source and receiver and homogeneous body-wave scattering in 3D media, they obtained

$$A_C(t) \propto t^{-1} e^{-\omega t/2Q_C} \quad [1]$$

where A_C is the coda amplitude at time t (from the earthquake origin time) and angular frequency ω. Q_C is termed the coda Q, and there has been some uncertainty regarding its physical meaning, in particular whether it describes intrinsic attenuation, scattering attenuation, or some combination of both. I will discuss this more later in the context of more complete theories. Regardless of its interpretation, this formula has proven successful in fitting coda decay rates in a large number of studies.

Single-scattering theory has also been important for modeling deep-Earth scattering in terms of random heterogeneity models, including interpretation of PKP precursor observations (e.g., Doornbos, 1976; Haddon and Cleary, 1974), PP precursors (King et al., 1975), P′P′ precursors (Vinnik, 1981), P_{diff} coda (Earle and Shearer, 2001), and PKiKP coda (Vidale and Earle, 2000). Born theory has also been used to model expected travel-time variations in direct arrivals that travel through random velocity heterogeneity (e.g., Baig and Dahlen, 2004a,b; Baig et al., 2003; Spetzler and Snieder, 2001). Although my focus in this chapter is largely on incoherent scattering from random media, it should be noted that the Born approximation can also be used to model the effect of specific velocity structures, provided their perturbations are weak compared to the background velocity field. In this case, true synthetic seismograms can be computed, not just the envelope functions. For example, Dalkolmo and Friederich (2000) recently used this approach to model the effect of several different hypothesized velocity anomalies near the core–mantle boundary (CMB) on long-period P waves. In addition, Born theory forms the basis for computing sensitivity kernels in finite-frequency tomography methods (e.g., Dahlen et al., 2000; Nolet et al., 2005).

1.24.2.1.1 Q notation and definitions

Coda Q, intrinsic Q, and scattering Q will be termed Q_C, Q_I, and Q_{Sc}, respectively. P-wave and S-wave Q are termed ${}^{\alpha}Q$ and ${}^{\beta}Q$, respectively. These can be combined so that, for example, ${}^{\beta}Q_I$ is intrinsic S-wave Q. This convention eliminates any chance of confusing shear-wave Q and scattering Q (both have sometimes been termed Q_S). The transmission Q, Q_T, describes the total attenuation (both intrinsic and scattering) suffered by the direct wave

$$Q_T^{-1} = Q_I^{-1} + Q_{Sc}^{-1} \quad [2]$$

and the amplitude reduction of the transmitted pulse for a constant Q_T medium is

$$A(t) = A_0 e^{-\omega t/2Q_T} \quad [3]$$

where A_0 is the amplitude of the pulse at $t=0$ and we have ignored any geometric spreading.

The scattering coefficient, g, is defined as the scattering power per unit volume (e.g., Sato, 1977) and has units of reciprocal length. The total scattering coefficient, g_0, is defined as the average of g over all directions and can also be expressed as

$$g_0 = l^{-1} = Q_{Sc}^{-1} k \quad [4]$$

where l is the mean free path and k is the wave number. One common way to estimate g_0 for S waves has been to compare the energy in the S coda to the total radiated S energy. Finally, following Wu (1985), we define the seismic albedo as the ratio of scattering attenuation to total attenuation

$$B_0 = \frac{Q_{Sc}^{-1}}{Q_{Sc}^{-1} + Q_I^{-1}} = \frac{g_0}{g_0 + Q_I^{-1} k} \quad [5]$$

These definitions of Q, g_0, and B_0 are general and can be applied to the multiple-scattering theories discussed later in this chapter.

1.24.2.2 Finite-Difference Calculations and the Energy-Flux Model

Finite-difference methods provide a direct, albeit computationally intensive, solution to the seismic wave equation for media of arbitrary complexity, and they (together with the finite element method) have become one of the most widely used techniques in seismology. Their earliest applications to study scattering involved modeling surface-wave and body-to-surface-wave scattering from surface topography, sediment-filled basins, and other buried interfaces (e.g., Levander and Hill, 1985). Here, I will discuss only their use in modeling body-wave scattering in random media. Reviews of this topic are contained in Frankel (1990) and Sato and Fehler (1998, 2012).

As computing power has improved, finite-difference simulations have progressed from the 2D parabolic approximation, to 2D using the full wave equation, to full 3D synthetics. The parabolic approximation considers only forward scattering and is useful when the heterogeneity correlation length is large compared to the seismic wavelength. Complete finite-difference simulations in 2D random media have been performed by Frankel and Clayton (1984, 1986), McLaughlin et al. (1985), McLaughlin and Anderson (1987), Frankel and Wennerberg (1987), Gibson and Levander (1988), Roth and Korn (1993), and Saito et al. (2003). Frenje and Juhlin (2000) computed both 2D and 3D finite-difference simulations. Hong and Kennett (2003), Hong (2004), and Hong et al. (2005) used a wavelet-based numerical approach to compute 2D synthetics for random media and Hong and Wu (2005) computed 2D synthetics for anisotropic models.

The Frankel studies provided key results in formulating the influential energy-flux model (EFM) of seismic coda (Frankel and Wennerberg, 1987) so I will describe them in some detail. Frankel and Clayton (1986) modeled teleseismic P-wave travel-time variations with a ~1 Hz plane wavelet vertically incident on a layer 150 km wide by 55 km thick, with a finite-difference grid spacing of 500 m. They found that observed travel-time variations of about 0.2 s (RMS) among stations spaced 10–150 km apart could be explained with 5% RMS random P-velocity variations, provided the correlation length was 10 km or greater. Frankel and Clayton (1986) also modeled high-frequency coda from local earthquakes using a ~20 Hz explosive source at the bottom corner of a layer 8 km long by 2 km thick. They found that the amplitude of high-frequency coda depends strongly on the presence of high wave number velocity perturbations. Gaussian and exponential models with correlation lengths of 10 km or greater (required to fit observed teleseismic travel-time variations) do not have sufficient small-scale structure to produce observed levels of

high-frequency coda. In contrast, a self-similar random medium model with a correlation distance of at least 10 km and RMS velocity variations of 5% can account for both sets of observations.

By measuring peak amplitude versus distance in their synthetics, Frankel and Clayton (1986) estimated Q for their random medium. Because their finite-difference calculation did not contain any intrinsic attenuation, this represents a measure of scattering Q (Q_{Sc}). The predicted attenuation (Q^{-1}) peaks at ka values between 1 and 2 for Gaussian random media and between about 1 and 6 for exponential random media. This is consistent with the strongest scattering occurring when the seismic wavelength is comparable to the size of the scatterers. However, attenuation is constant with frequency for self-similar random media, as expected since the velocity fluctuations have equal amplitudes over a wide range of scales. Frankel and Clayton showed that these results were in rough agreement with those predicted by single-scattering theory in two dimensions (to match the geometry of the finite-difference simulations).

Frankel and Clayton (1986) also measured coda decay rates for finite-difference synthetics computed for sources within a 12 km by 12 km grid at 20 m spacing. They found that their observed coda decay rates were significantly less than those predicted by single-scattering theory in the case of moderate to large scattering attenuation ($Q_{Sc} \leq 200$), indicating that multiple scattering is contributing a substantial portion of the coda energy. This implies that in these cases, coda Q (Q_C) as determined from coda falloff and the single-scattering model of coda (e.g., Aki and Chouet, 1975) does not provide a reliable estimate of transmission Q.

Motivated by these finite-difference results and the limitations of the single-scattering model of coda generation, Frankel and Wennerberg (1987) introduced what they termed the EFM of coda. This phenomenological model is based on the idea that the coda energy behind the direct wave front can be approximated as homogeneous in space. This observation had previously been reported for microearthquake coda for lapse times more than twice the S-wave travel time (e.g., Aki, 1969; Rautian and Khalturin, 1978), and Frankel and Wennerberg (1987) showed that it also could be seen in finite-difference synthetics (see **Figure 2**). It implies that at sufficiently long times, the coda amplitude at all receivers is approximately the same (scaling only with the magnitude of the source), regardless of the source–receiver distance. The EFM permits the time decay of the coda amplitude to be modeled very simply and to separate the effects of scattering and intrinsic attenuation in the medium.

By considering the energy density of the coda uniformly distributed in an expanding volume behind the direct wave front, Frankel and Wennerberg derived an expression for the predicted time decay of the coda amplitude

$$A_C(t) \propto t^{-3/2} e^{-\omega t/2Q_I} \sqrt{1 - e^{-\omega t/Q_{Sc}}} \quad [6]$$

where t is time, ω is angular frequency, Q_I^{-1} is intrinsic attenuation, and Q_{Sc}^{-1} is scattering attenuation. For short time and/or high Q_{Sc} (i.e., weak scattering, tQ_{Sc}^{-1} is very small), this equation reduces to

$$A_C(t) \propto t^{-1} e^{-\omega t/2Q_I} \quad [7]$$

This is equivalent to the Aki and Chouet (1975) expression (eqn [1]) for the single-scattering model, assuming coda Q and intrinsic Q are equivalent ($Q_C = Q_I$). This agrees with the original interpretation of Q_C given by Aki and Chouet (1975) and contradicts the Aki (1980) statement that in the context of single-scattering theory, Q_C should be considered as an effective Q that includes both absorption and scattering effects. Frankel and Wennerberg (1987) showed that the EFM predicts the amplitude and coda decay observed in finite-difference synthetics for random media with a wide range of scattering Q and is more accurate than the single-scattering model for media with moderate to strong scattering attenuation ($Q_{Sc} \leq 150$). Finally, they used the EFM to estimate Q_{Sc} and Q_I from the coda of two $M \sim 3$ earthquakes near Anza, California.

There have been numerous other studies that have attempted to resolve Q_{Sc} and Q_I from local earthquake coda (e.g., Cirerone et al., 2011; Fehler et al., 1992; Jemberie and Nyblade, 2009; Mayeda et al., 1991; Padhy and Subhadra, 2010; Padhy et al., 2011; Toksöz et al., 1988; Wu and Aki, 1988). Notable are Mayeda et al. (1992), who analyzed S-wave coda from Hawaii, Long Valley, and central California. They found a complicated relationship between theoretical predictions and observed Q_C, Q_{Sc}, and Q_I and argued that models with depth-dependent scattering and intrinsic attenuation are necessary to explain their results.

The EFM was developed to explain local earthquake coda and finite-difference simulations of spherical wave fronts in media with uniform scattering. It is not directly applicable to modeling teleseismic coda because of the strong concentration of scattering in the crust and lithosphere compared to much weaker scattering deeper in the mantle. This has motivated the development of extended EFMs involving the response of one or more scattering layers to a wave incident from below (e.g., Korn, 1988, 1990, 1997; Langston, 1989).

The resulting formulas for the coda decay rate are more complicated than the simple EFM because they depend upon several additional parameters, including the travel time through the layer and the amount of leakage back into the half-space. Korn (1988) developed the theory for a spherical wave with a cone of energy incident upon a scattering zone

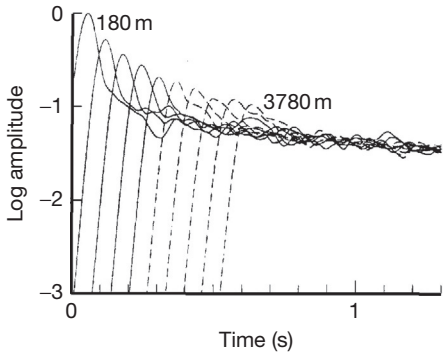

Figure 2 Envelopes of finite-difference synthetic seismograms for receivers at distances of 180–3780 m from the source as computed by Frankel and Wennerberg (1987) for a random medium with a correlation distance of 40 m. Note that the envelopes decay to a common level following the initial pulse, indicating spatial homogeneity of coda energy.

and used it to model regional earthquakes recorded by the Warramunga array in Australia. Langston (1989) developed a scattering layer-over-half-space model and showed that it was consistent with coda decay in teleseismic P waves recorded at two stations (named PAS and SCP) in the United States. Korn (1990) tested a scattering layer over homogenous half-space EFM using a 2D acoustic finite-difference code and found that it gave reliable results for both weak and strong scattering regimes. Korn (1997) further extended the EFM to explicitly include depth-dependent scattering and showed that it gave reliable results when compared to synthetics computed for a 2D elastic (P–SV) finite-difference code.

Wagner and Langston (1992a) computed 2D acoustic and elastic finite-difference synthetics for upcoming P waves incident on 150 different models of heterogeneous layers over a homogeneous half-space. These models varied in their layer thickness, random heterogeneity correlation length (different vertical and horizontal correlation lengths were allowed), and RMS velocity heterogeneity. They found that the scattering attenuation of the direct pulse depends upon ka and is strongest for spatially isotropic heterogeneity, in which case most of the coda energy was contained in low apparent velocity S waves and surface waves. In contrast, anisotropic models with horizontally elongated heterogeneities produce coda with mostly vertically propagating layer reverberations.

More recent finite-difference calculations for random media include the 2D whole-Earth pseudospectral calculations of Furumura et al. (1998) and Wang et al. (2001), Thomas et al. (2000) who computed 2D whole-Earth acoustic synthetics to model PKP precursors, Cormier (2000) who used a 2D elastic pseudospectral method to model the effects of D'' heterogeneity on the P and S wavefields, Korn and Sato (2005) who compared 2D finite-difference calculations with synthetics based on the Markov approximation, and Jahnke et al. (2008) who developed an axisymmetric finite-difference code suitable for parallel computers and showed how it can be used to model whole-mantle scattering at frequencies up to 0.4 Hz.

1.24.2.3 Multiple-Scattering Theories

If the energy in the scattered wavefield is a significant fraction of the energy in the direct wave, then the Born approximation is inaccurate and a higher-order theory should be used that takes into account the energy reduction in the primary wave and the fact that the scattered waves may experience more than one scattering event. These effects are all naturally accounted for using the finite-difference calculations discussed earlier, but these are computationally intensive and there is a need for faster approaches that also provide physical insight into the scattering process. In the case of very strong scattering, the diffusion equation can be applied by assuming a random walk process. Although this approach preserves energy, it violates causality by permitting some energy to arrive before the direct P wave. The first applications of the diffusion equation in seismology include the coda-wave analyses of Wesley (1965) and Aki and Chouet (1975) and the lunar seismogram studies of Nakamura (1977), Dainty and Toksöz (1977), and Dainty and Toksöz (1981).

At large times and small distances from the source, the diffusion equation predicts that the coda amplitude varies as

$$A(t) \propto t^{-3/4} e^{-\omega t/2Q_I} \quad [8]$$

where Q_I is the intrinsic attenuation. Notice that Q_{Sc} does not appear in this equation because the exact level of scattering is not important provided it is strong enough that the energy is obeying a random walk process. The diffusion equation can also be used to model the case of a strong scattering layer over a homogeneous half-space (e.g., Dainty et al., 1974; Margerin et al., 1998, 1999; Wegler, 2004), in which case an additional decay term exists to account for the energy leakage into the half-space.

Another approach to modeling multiple scattering is to sum higher-order scattered energy, and the predicted time dependence of scattered energy was obtained in this way for double-scattering (Kopnichev, 1977) and multiple scattering up to seventh order (Gao et al., 1983a,b). Hoshiba (1991) used a Monte Carlo approach (see the succeeding text) to correct and extend these results to tenth-order scattering. Richards and Menke (1983) performed numerical experiments on 1D structures with many fine layers to characterize the effects of scattering on the apparent attenuation of the transmitted pulse and the relative frequency content of the direct pulse and its coda.

Most current approaches to synthesizing multiple scattering use radiative transfer theory to model energy transport. Radiative transfer theory was first used in seismology by Wu (1985) and Wu and Aki (1988), and recent reviews of the theory are contained in Sato and Fehler (1998, 2012) and Margerin (2004). Other results are detailed in Shang and Gao (1988), Zeng et al. (1991), Sato (1993), and Sato et al. (1997). Sato and Nishino (2002) used radiative transfer theory to model multiple Rayleigh-wave scattering. Analytic solutions are possible for certain idealized cases (e.g., Sato, 1993; Wu, 1985; Zeng, 1991), but obtaining general results requires extensive computer calculations.

Two analytic results are of particular interest (and can be used as tests of numerical simulations). For the case of no intrinsic attenuation, Zeng (1991) showed the coda power converges to the diffusion solution at long lapse times

$$P_C(t) \propto t^{-3/2} \quad [9]$$

For elastic waves with no intrinsic attenuation, the equilibrium ratio of P and S energy density is given by (e.g., Papanicolaou et al., 1996; Ryzhik et al., 1996; Sato, 1994)

$$E_P/E_S = \frac{1}{2}(\beta/\alpha)^3 \quad [10]$$

Assuming a Poisson solid, this predicts about ten times more S energy than P energy at equilibrium, a result of the relatively low efficiency of S-to-P scattering compared to P-to-S scattering (e.g., Malin and Phinney, 1985; Zeng, 1993). For media with intrinsic attenuation, an equilibrium ratio also exists but will generally differ from the purely elastic case (Margerin et al., 2001a,b). Shapiro et al. (2000) showed that this ratio can be estimated from the divergence and curl of the displacement as measured with a small-aperture array and that its stability with time provides a test of whether the coda is in the diffusive regime.

Equation [10] is only valid for scattering within a uniform whole space and somewhat lower E_S/E_P ratios are expected at the surface of a uniform half-space. Margerin et al. (2009)

examined energy partitioning of seismic coda at Piñon Flat Observatory in California and obtained an average E_S/E_P ratio of about 2.8, over two times smaller than the expected value of 7.2 for equilibrium partitioning at the surface of a Poisson half-space. They explained their results by developing a theory of energy partitioning in a layered media and showed that E_S/E_P drops near the resonant frequency of a surface low-velocity layer. Thus, observations of equilibrium E_S/E_P ratios can provide information on local Earth structure. Margerin (2013) provided a theoretical treatment of multiple scattering and energy partitioning from randomly distributed point scatterers, which includes the effects of strong resonant scattering.

Wu (1985) used radiative transfer theory to address the problem of separating scattering from intrinsic attenuation. He showed that the coda energy density versus distance curves have different shapes depending upon the seismic albedo, B_0 (see eqn [5]), and thus, in principle, it is possible to separate scattering and intrinsic Q by measuring energy density distribution curves. Hoshiba (1991) pointed out that in practice, the use of finite window lengths for measuring coda will lead to underestimating the total energy (compared to the infinite lapse-time windows in Wu's theory), likely biasing the resulting estimates of seismic albedo. To deal with this problem, Fehler et al. (1992) introduced the multiple lapse-time window (MLTW) analysis, which measures the energy in consecutive time windows as a function of epicentral distance. The MLTW approach has been widely used in studies of S coda (see the succeeding text).

A powerful method for computing synthetic seismograms based on radiative transfer theory is to use a computer-based Monte Carlo approach to simulate the random walk of millions of seismic energy 'particles,' which are scattered with probabilities derived from random media theory. **Figure 3** illustrates a simple example of this method applied to 2D isotropic scattering. Variations on this basic technique are described by Gusev and Abubakirov (1987), Abubakirov and Gusev (1990), Hoshiba (1991, 1994, 1997), Margerin et al. (2000), Bal and Moscoso (2000), Yoshimoto (2000), Margerin and Nolet (2003a,b), and Shearer and Earle (2004). Because of the potential of the Monte Carlo method for modeling whole-Earth, high-frequency scattering, these results are now summarized in some detail.

Gusev and Abubakirov (1987) used the Monte Carlo method to model acoustic-wave scattering in a whole space and considered both isotropic scattering and forward scattering with a Gaussian angle distribution. They parameterized the scattering in terms of a uniform probability per unit volume, resulting in an exponential distribution of path lengths. Intrinsic attenuation was not included. They showed that their results agree with the diffusion model for large lapse times. Abubakirov and Gusev (1990) described in detail this method and its application to model S coda from Kamchatka earthquakes. They obtained an S-wave mean free path for the Kamchatka lithosphere of 110–150 km over a 1.5–6 Hz frequency range.

Hoshiba (1991) modeled the spherical radiation of S-wave energy in a constant velocity medium using a Monte Carlo simulation that included isotropic scattering with uniform probability. He showed that the results agreed with single-scattering theory for weak scattering (i.e., travel distances

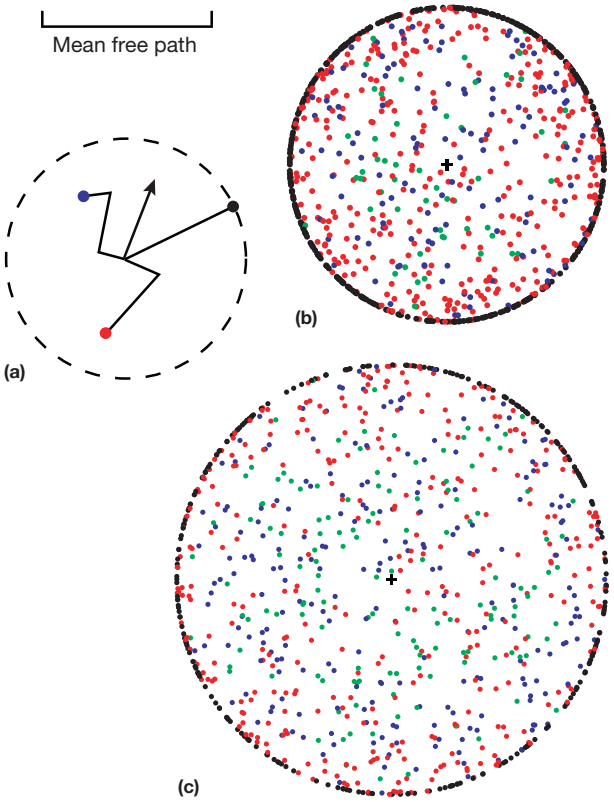

Figure 3 Example of a Monte Carlo computer simulation of random scattering of seismic energy particles, assuming 2D isotropic scattering in a uniform whole space. Particles are sprayed in all directions from the source with constant scattering probability defined by the indicated mean free path length, l. As indicated in (a), black dots show particles that have not been scattered, red dots show particles that have scattered once, blue dots show particles that have scattered twice, and green dots show particles scattered three or more times. (b) Results for 1000 particles after $t = 0.8/v$, where v is velocity. (c) Results for 1000 particles after $t = 1.25/v$. Note that the particle density is approximately constant for the scattered energy inside the circle defining the direct wave front, as predicted by the energy-flux model.

$<10\%$ of the mean free path) and agreed with the diffusion model for strong scattering (i.e., travel distances more than ten times longer than the mean free path). Hoshiba (1991) was able to use his Monte Carlo results to correct and extend the multiple-scattering terms of Gao et al. (1983a,b). He found that his simulations at long lapse times were consistent with the radiative transfer theory of Wu (1985) but that reliable estimates of seismic albedo are problematic from short time windows. Finally, Hoshiba (1991) showed that for multiple scattering, coda Q is much more sensitive to intrinsic Q than to scattering Q (as was argued by Frankel and Wennerberg, 1987, on the basis of the EFM).

Wennerberg (1993) considered the implications of lapse time-dependent observations of Q_C and methods for separating intrinsic and scattering attenuation with respect to the single-scattering model, Zeng's (1991) multiple-scattering model, Hoshiba's (1991) model, and Abubakirov and Gusev's (1990) results. Hoshiba (1994) extended his Monte Carlo method to consider depth-dependent scattering strength and intrinsic attenuation, and Hoshiba (1997) included the

effects of a layered velocity structure to model local earthquake coda at distances up to 50 km. Hoshiba simulated SH-wave reflection and transmission coefficients at layer interfaces as probabilities of reflection or transmission of particles in the Monte Carlo method but did not include P waves and the conversions between P and S waves. The results showed that coda amplitudes depend upon the source depth even late into the coda.

Margerin et al. (1998) applied the Monte Carlo approach to a layer over a half-space model, representing the crust and upper mantle, and included both surface- and Moho-reflected and transmitted phases. As in Hoshiba (1997), reflection and transmission coefficients are converted to probabilities for the individual particles. S waves only are modeled (using the scalar-wave approximation, i.e., no P-to-S conversions) and no intrinsic attenuation is included. Margerin et al. (1998) compared their numerical results in detail with solutions based on the diffusion equation and found good agreement for suitable mean free path lengths. They point out the importance of the crustal waveguide for trapping energy near the surface and that the possibility of energy leakage into the mantle should be taken into account in calculations of seismic albedo.

Bal and Moscoso (2000) explicitly included S-wave polarization and showed that S waves become depolarized under multiple scattering. Yoshimoto (2000) introduced the direct simulation Monte Carlo method, which uses a finite-difference scheme for ray tracing and can thus handle velocity models of arbitrary complexity, including lateral varying structures. However, intrinsic attenuation and directional scattering were not included. Yoshimoto showed that a velocity increase with depth strongly affects the shape of the coda envelope, compared with uniform velocity models, and that it is important to properly model energy that may be trapped at shallow depths.

Margerin et al. (2000) extended the Monte Carlo approach to elastic waves, taking into account P-to-S conversions and S-wave polarization. They considered scattering from randomly distributed spherical inclusions within a homogeneous background material, using the solutions of Wu and Aki (1985a). For both Rayleigh scatterers (spheres much smaller than the seismic wavelength) and Rayleigh–Gans scatterers (spheres comparable to the seismic wavelength), they found good agreement with single-scattering theory at short times and with the diffusion equation solution at long times. In addition, the P-to-S energy density ratio and the coda decay rate at long times converged to their theoretical expected values.

Margerin and Nolet (2003a,b) further extended the Monte Carlo approach to model whole-Earth wave propagation and scattering. They showed that their Monte Carlo synthetics for the PKP AB and BC branches produced energy versus distance results in good agreement with geometric ray theory. They computed scattering properties based on random media models characterized by velocity perturbations with an exponential correlation length. For whole-mantle scattering, they found that the Born approximation is only valid up to mean free paths of about 400 s, corresponding to 0.5% RMS velocity perturbations. They also applied their method to model PKP precursor observations; these results will be discussed later in this chapter.

Shearer and Earle (2004) implemented a particle-based Monte Carlo method for computing whole-Earth scattering. They included both P and S waves radiated from the source, mode conversions, S-wave polarizations, and intrinsic attenuation. For a simple whole-space model, they showed that their approach agreed with theoretical results for the S/P energy ratio and expected t^{-15} falloff in power at large times. For modeling the whole Earth, they included the effects of reflection and transmission coefficients at the free surface, Moho, CMB, and inner-core boundary (ICB). Scattering probabilities and scattering angles were computed assuming random velocity and density variations characterized by an exponential ACF. They applied this method to model the time and distance dependence of high-frequency P coda amplitudes (see **Section 1.24.3.2**).

Wegler et al. (2006), Przybilla et al. (2006), and Przybilla and Korn (2008) compared Monte Carlo solutions using the elastic radiative transfer equations to 3D finite-difference calculations and found good agreement in envelope shapes, including peak amplitudes, envelope broadening, and coda decay rates. However, Przybilla and Korn (2008) documented an interesting breakdown in radiative transfer results based on the Born scattering coefficients in the vicinity of a point source, where waveform modeling shows that even for a pure compressional source, there is some fraction of shear-wave energy generated by near-source scattering that is missed in Born approximation calculations.

All of these results suggest that body-wave scattering in the whole Earth can now be reasonably well modeled using ray theory and particle-based Monte Carlo methods. Although somewhat computationally intensive, continued improvements in computer speed make them practical to run on modest machines. They can handle multiple scattering over a range of scattering intensities, bridging the gap between the Born approximation for weak scattering and the diffusion equation for strong scattering. They also can include general depth-dependent or even 3D variations in scattering properties, including non-isotropic scattering, without a significant increase in computation time compared to simpler problems.

1.24.2.4 Other Theoretical Methods

Lerche and Menke (1986) presented an inversion method to separate intrinsic and scattering attenuation for a plane-layered medium. Gusev (1995) and Gusev and Abubakirov (1999a,b) developed a theory for reconstructing a vertical profile of scattering strength from pulse broadening and delay of the peak amplitude. Saito et al. (2002, 2003) modeled envelope broadening in S waves by applying the parabolic approximation to a von Karman random medium. Sato et al. (2004) extended this approach to develop a hybrid method for synthesizing whole-wave envelopes that uses the envelope obtained from the Markov approximation as a propagator in the radiative transfer integral and showed that the results agreed with finite-difference calculations. Takahashi (2012) also used the Markov approximation to model wide-angle scattering of S waves in northeastern Japan and the time delays in their maximum amplitudes.

The effect of anisotropic random media (where the scattering properties depend upon the angle of the incident wave)

was considered numerically by Wagner and Langston (1992a) and Roth and Korn (1993) and theoretically by Müller and Shapiro (2003), Hong and Wu (2005), and Margerin (2006). Recent work on using small-aperture seismic arrays on coda energy to constrain the directions of individual scatterers includes Schisselé et al. (2004) and Matsumoto (2005).

1.24.3 Scattering Observations

Seismic scattering within the Earth is mainly observed in the incoherent energy that arrives between the direct seismic phases, such as P, S, and PKP. In addition, occasionally specific scatterers can be imaged using seismic arrays. Scattering can also influence the direct phases through amplitude reduction and pulse broadening, effects characterized by the scattering attenuation parameter, Q_{Sc}^{-1}. In this way, studies of seismic attenuation are also resolving scattering, although they often do not attempt to separate intrinsic and scattering attenuation. The incoherent scattered seismic wavefield usually follows a direct seismic arrival and is termed the *coda* of that phase (e.g., P coda and S coda), but occasionally, the ray geometry is such that scattered energy can arrive before a direct phase (e.g., PKP precursors). These precursory arrivals are particularly valuable for studying deep-Earth scattering because they are less sensitive to the strong scattering in the lithosphere. Scattering is usually studied at relatively high frequencies (1 Hz or above) where coda is relatively strong and local earthquake records have their best signal-to-noise ratio.

S-wave coda from local and regional events has been the focus of many studies, has motivated much of the theoretical work, and continues to be an active field of research. Here, I will briefly review S coda studies and their implications for scattering in the crust and lithosphere but will devote more attention to other parts of the scattered seismic wavefield, which provide better constraints on deep-Earth structure. Previous review articles that discuss deep-Earth scattering include Bataille et al. (1990) and Shearer et al. (1998). **Figure 4** shows where much of the scattered energy arrives with respect to travel-time curves for the major seismic phases. In principle, any seismic phase that travels through the lower mantle or the CMB will be sensitive to deep-Earth scattering. Although separating deep scattering effects from crust and lithospheric scattering can be challenging, this is possible in some cases, either

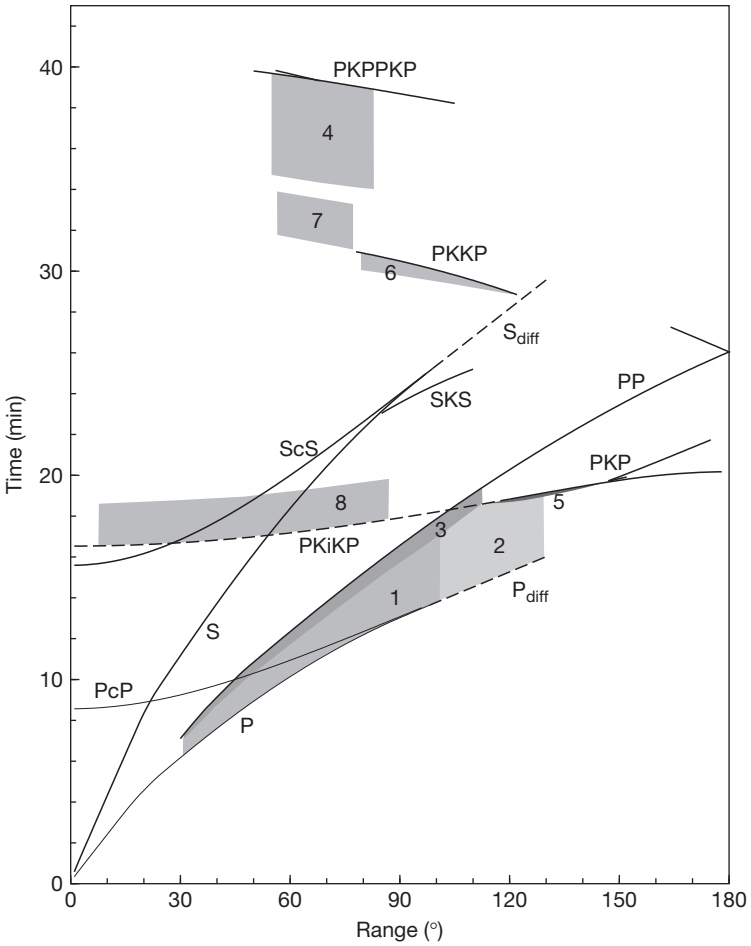

Figure 4 Travel-time curves for teleseismic body waves and some of the regions in the short-period wavefield that contain scattered arrivals. These include (1) P coda, (2) P_{diff} coda, (3) PP precursors, (4) P′P′ precursors, (5) PKP precursors, (6) PKKP precursors, (7) $PKKP_X$, and (8) PKiKP coda. The plotted boundaries are approximate.

from a fortunate ray geometry or by careful comparison of coda amplitudes at different distances or between different phases.

The picture that is emerging from these studies is that seismic scattering from small-scale velocity perturbations is present throughout the Earth, with the exception of the fluid outer core. However, the exact strength, scale length, depth dependence, and lateral variability of the scattering remain unresolved, particularly in the vicinity of the core–mantle and ICBs, where they may also be contributions from topographic irregularities or boundary layer structure.

1.24.3.1 Local and Regional S Coda

S coda measurements are of two main types: (1) those that simply fit the coda decay rate and estimate ${}^{\beta}Q_C$ without attempting to separate scattering and intrinsic attenuation and (2) those that measure energy density and estimate the scattering coefficient g_0 (or its reciprocal, the mean free path). The latter studies typically obtain a separate estimate for intrinsic attenuation and thus can compute the seismic albedo, B_0. The basic relationships among these parameters are given in eqns [4] and [5]. In both types of studies, frequency dependence can also be examined by filtering the data in different bands.

Coda Q studies include Rautian and Khalturin (1978), Roecker et al. (1982), Rodriguez et al. (1983), Singh and Herrmann (1983), Biswas and Aki (1984), Pulli (1984), Rhea (1984), Jin et al. (1985), Del Pezzo et al. (1985), Jin and Aki (1988), van Eck (1988), Kvamme and Havskov (1989), Matsumoto and Hasegawa (1989), Baskoutas and Sato (1989), Oancea et al. (1991), Tsuruga et al. (2003), Giampiccolo et al. (2004), and Goutbeek et al. (2004).

Reviews of Q_C measurements include Herraiz and Espinoa (1987), Matsumoto (1995), and Sato and Fehler (1998, 2012). In general, Q_C is frequency-dependent and increases from about 100 at 1 Hz to 1000 at 20 Hz (i.e., there is less attenuation at higher frequencies). However, there are regional variations of about a factor of ten and typically Q_C is lower in tectonically active areas and higher in stable regions, such as shields. As discussed previously, how to interpret Q_C in terms of Q_{Sc} and Q_I has been the subject of some debate, and it is becoming increasingly clear that depth-dependent calculations (which include variations in the background velocity, the scattering characteristics, and the intrinsic attenuation) are required in many cases to fully describe coda observations.

Some studies (e.g., Akamatsu, 1991; Gagnepain-Beyneix, 1987; Giampiccolo et al., 2004; Goutbeek et al., 2004; Gupta et al., 1998; Kosuga, 1992; Kvamme and Havskov, 1989; Rautian and Khalturin, 1978; Roecker et al., 1982; Singh et al., 2001) have observed that Q_C increases with increasing lapse time (i.e., eqn [1] does not fit the entire coda envelope), suggesting that the later part of the coda contains energy that propagated through less attenuating material than the early part of the coda. Gusev (1995) showed that an increase in Q_C with time in the coda is predicted from a single isotropic scattering model in which Q_{Sc} increases with depth. Margerin et al. (1998) applied radiative transfer theory to show that a model of scattering in the crust above much weaker scattering in the mantle predicts Q_C values that depend upon the reflection coefficient at the Moho, implying that energy leakage into the mantle has implications for the interpretation of coda Q.

Following Sato and Fehler (1998, 2012), we may divide scattering attenuation estimates into those obtained using the single-scattering model and those based on the MLTW analysis. Single-scattering studies include Sato (1978), Aki (1980), Pulli (1984), Dainty et al. (1987), Kosuga (1992), and Baskoutas (1996). Multiple lapse-time studies are summarized in **Figure 5** and include Fehler et al. (1992), Mayeda et al. (1992), Hoshiba (1993), Jin et al. (1994), Akinci et al. (1995), Canas et al. (1998), Ugalde et al. (1998, 2002), Hoshiba et al. (2001), Bianco et al. (2002, 2005), Vargas et al. (2004), Goutbeek et al. (2004), Mukhopadhyay and Tyagi (2008), Badi et al. (2009), Chung et al. (2010), Carcolé and Sato (2010), Lee et al. (2010), and Del Pezzo et al. (2011). Values of the coefficient go for S-to-S scattering range from about 0.002 to 0.05 km^{-1} (mean free paths of 20–500 km) for frequencies between 1 and 30 Hz. Some papers (e.g., Bianco et al., 2005; Goutbeek et al., 2004; Hoshiba, 1993; Jin et al., 1994; Mayeda et al., 1992) have found a frequency dependence in the seismic albedo and among different regions, but in general, this dependence is not as consistent as that seen in Q_C studies. Several recent papers noted the importance of considering depth-dependent velocity structure in computing scattering attenuation (e.g., Bianco et al., 2002, 2005; Hoshiba et al., 2001).

Lacombe et al. (2003) modeled S coda in France at epicentral distances between 100 and 900 km using acoustic radiative transfer theory applied to a two-layer model. They found that a model with scattering confined to the crust and uniform intrinsic attenuation could explain their data at 3 Hz but that the trade-off between scattering and intrinsic attenuation was too strong to reliably determine the relative contribution of each

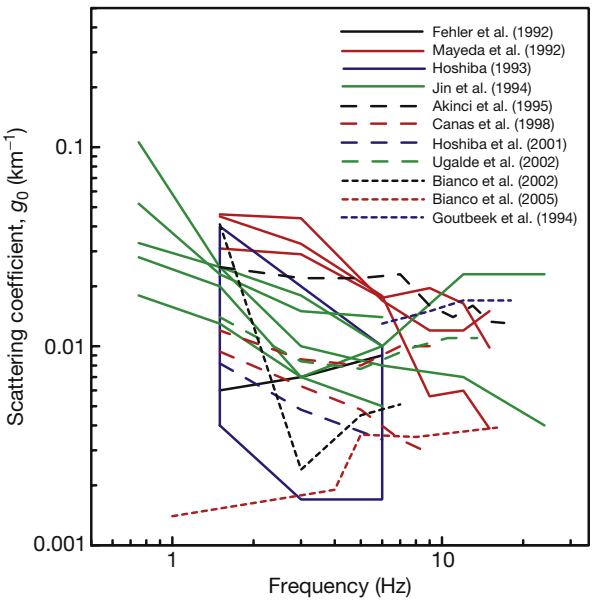

Figure 5 A summary of observations of the total scattering coefficient g_0 for S-wave scattering versus frequency, obtained using the multiple lapse-time window (MLTW) method. Results from various studies around the world are indicated with different colors.

parameter. At the regional epicentral distances of their model, the crustal waveguide had a dominating effect on the S coda.

Carcolé and Sato (2010) applied the MLTW analysis to the over 700 stations of the Japanese Hi-net seismic network to obtain high-resolution maps of both scattering and intrinsic attenuation, which show strong regional variations. In general, northeast Japan has stronger scattering than southwest Japan at 1–2 Hz, with the strongest scattering occurring near the volcanic arcs. In general, scattering and intrinsic attenuation variations are correlated and strong scattering and high intrinsic attenuation are often seen in areas where low seismic velocity anomalies have been observed in other studies. The Carcolé and Sato (2010) results agree reasonably well with the earlier work of Hoshiba (1993) for common stations, but the much greater Hi-net station density permits much more detailed mapping of scattering structure.

In addition to the S coda decay rates at relatively long lapse times used to determine coda Q, there are other aspects of the coda that provide additional constraints on scattering. The complete seismogram envelope can be studied, including the broadening of the direct S envelope and the delay in its peak amplitude (e.g., Obara and Sato, 1995; Sato, 1989, 1991; Scherbaum and Sato, 1991). Deviations from the average coda decay rate for a number of stations can be inverted to construct a 3D model of scattering intensity in the crust and upper mantle (e.g., Chen and Long, 2000; Nishigami, 1991, 1997; Obara, 1997; Taira and Yomogida, 2004). Similar methods were used by Revenaugh (1995, 1999, 2000) to back-project P coda recorded in southern California and by Hedlin and Shearer (2000) to invert PKP precursor amplitudes (see the succeeding text). Periodic rippling of SH coda envelopes in northeastern Japan was noted by Kosuga (1997) who suggested this may be caused by trapped waves within a low-velocity layer in the top part of the subducting slab.

Spudich and Bostwick (1987) showed how Green's function reciprocity can be used to obtain information about the ray takeoff directions from the earthquake source region, using a cluster of earthquakes as a virtual array. Applying this method to aftershocks of the 1984 Morgan Hill earthquake in California, they found that the early S coda was dominated by multiple scattering within 2 km of each seismic station. Scherbaum et al. (1991) used this approach to study two microearthquake clusters in northern Switzerland and found that the early S coda contained energy leaving the source at close to the same angle as the direct wave but that the later (at least 1.5–2 times the S travel time) coda contains energy from waves leaving the source in a variety of directions. Spudich and Miller (1990) and Spudich and Iida (1993) showed how an interpolation approach using distributed earthquake sources can be used to estimate scattering locations in the vicinity of the 1986 North Palm Springs earthquake in California.

Hong and Menke (2008) applied source-array analysis to regional recordings of nuclear explosions at the Balapan test site in Kazakhstan and identified coherent coda energy originating as *Rg* waves that lasts continuously to the end of the coda (more than 700 s) at 0.2–0.8 Hz. This suggests that *Rg*-to-*Rg* scattering is the main contributor to the low-frequency scattered wavefield. However, about 80% of the coda energy is composed of diffusive (multiplied scattered) waves.

1.24.3.2 P Coda

Local and many regional coda studies have mainly focused on the S-wave coda because of its higher amplitude and longer duration than P-wave coda (which is truncated by the S-wave arrival). However, at teleseismic distances, P waves and their coda are more prominent than S waves at high frequencies because of the severe effect of mantle attenuation on the shear waves. A number of studies both from single stations and arrays have attempted to resolve the origin of the scattered waves in the P coda and to distinguish between near-source scattering and near-receiver scattering.

Aki (1973) modeled scattering of P waves beneath the Montana Large Aperture Seismic Array (LASA) using Chernov single-scattering theory. At 0.5 Hz, he achieved a good fit to the data with a random heterogeneity model extending to 60 km depth beneath LASA, with RMS velocity fluctuations of 4% and a correlation distance of 10 km. Stronger scattering at higher frequencies exceeded the validity limits of the Born approximation.

Frankel and Clayton (1986) compared teleseismic traveltime anomalies observed across the LASA and NORSAR, as well as very high-frequency coda ($f \geq 30$ Hz) observed for microearthquakes, to synthetic seismograms for random media generated using a finite-difference method. They found that a random medium with self-similar velocity fluctuations ($a \geq 10$ km) of 5% within an $\sim$100 km thick layer could explain both types of observations.

Dainty (1990) reviewed array studies of teleseismic P coda, such as that recorded by the LASA and NORES arrays. He distinguished between 'coherent' coda, which has nearly the same slowness and back azimuth as direct P, and 'diffuse' coda, which is characterized by energy arriving from many different directions. He argued that coherent coda is generated by shallow, near-source scattering in the crust, rather than deeper in the mantle, because it is absent or weak for deep-focus earthquakes. In contrast, the diffuse coda is produced by near-receiver scattering and has power concentrated at slownesses typical of surface shear waves (Lg). Lay (1987) showed that the dispersive character of the first 15 s of the P coda from nuclear explosions was due to near-source effects.

Gupta and Blandford (1983) and Cessaro and Butler (1987) addressed the question as to how scattering can cause transversely polarized energy to appear in P and P coda, an issue relevant to discrimination methods between earthquakes and explosions. Their observations at different distances and frequency bands suggested that both near-source and near-receiver scattering must be present. Flatté and Wu (1988) performed a statistical analysis of phase and amplitude variations of teleseismic P waves recorded by the NORSAR array. They fitted their results with a two-overlapping-layer model of lithospheric and asthenospheric heterogeneity beneath NORSAR, consisting of the summed contributions from a 0 to 200 km layer with a flat power spectrum and a 15–250 km layer with a k^{-4} power spectrum (the deeper layer corresponds to an exponential autocorrelation model with scale larger than the array aperture of 110 km). The RMS P-velocity variations are 1–4%. This model has relatively more small-scale scatterers in the shallow crust (which the authors attribute to clustered cracks or intrusions) and relatively more large-scale scatterers in the

asthenosphere (which the authors suggest may be temperature or compositional heterogeneities).

Langston (1989) studied teleseismic P waves recorded at station PAS in California and SCP in Pennsylvania. He showed that the coda amplitude cannot be explained by horizontally layered structures of realistic velocity contrasts and that 3D scattering is required. He could explain the observed coda decay by adopting the EFM of Frankel and Wennerberg (1987) for the case of a scattering layer above a homogenous half-space. He found that scattering is more severe at PAS than SCP, as indicated by higher coda levels and a slower decay rate, obtaining a scattering Q estimate for PAS of 239 (2 s period) compared to 582 for SCP.

Korn (1988) examined the P coda from Indonesian earthquakes recorded at the Warramunga array in central Australia and found that the coda energy decreased with increasing source depth. He computed the power in the coda at different frequency bands between 0.75 and 6 Hz and fitted the results with the EFM of Frankel and Wennerberg (1987). The results indicated frequency dependence in both intrinsic attenuation and scattering attenuation ($Q_I = 300$ at 1 Hz, increasing almost linearly with frequency above 1 Hz; $Q_{Sc} = 340$ at 1 Hz, increasing as $f^{0.85}$). Assuming random velocity fluctuations with an exponential ACF, results from Sato (1984) can be used to estimate that RMS velocity variations of 5% at 5.5 km scale length are consistent with the observed Q_{Sc} below the Warramunga array. Korn (1990) extended the EFM to accommodate a scattering layer over a homogeneous half-space (a modeling approach similar to that used by Langston, 1989) and applied the method to the short-period Warramunga array data of Korn (1988) for deep earthquakes. With the new model, he found an average scattering Q of 640 at 1 Hz for the lithosphere below the array and higher values of intrinsic Q, implying that diffusion rather than anelasticity is the dominant factor controlling teleseismic coda decay rates. Korn (1993) further applied this approach to teleseismic *P* coda observations from nine stations around the Pacific. He found significant differences in scattering Q among the stations ($Q_{Sc} = 100$–500). The observed frequency dependence of Q_{Sc} is in approximate agreement with single-scattering theory for random heterogeneities and favors von Karman type ACFs over Gaussian or self-similar models.

Bannister et al. (1990) analyzed teleseismic P coda recorded at the NORES array using both array and three-component methods. They resolved both near-source and near-receiver scattering contributions to coda, with the bulk of receiver-side scattering resulting from P-to-*Rg* conversions from two nearby areas (10 and 30 km away) with significant topography. Gupta et al. (1990) performed frequency–wave number analysis on high-frequency NORES data and identified both near-receiver P-to-*Rg* scattering and near-source *Rg*-to-P scattering. Dainty and Toksöz (1990) examined scattering in regional seismograms recorded by the NORES, FINES, and ARCES arrays. P coda energy was concentrated in the on-azimuth direction but appeared at different phase velocities, suggesting different contribution mechanisms.

Wagner and Langston (1992b) applied frequency–wave number analysis to P′P′ (PKPPKP) waves recorded by the NORES arrays for deep earthquakes. Most of the coda was vertically propagating, but an arrival about 15 s after the direct wave can be identified as body-to-Rayleigh-wave scattering from a point 30 km west-southwest of the array (this scattering location was previously identified in P-wave coda by Bannister et al. (1990) and Gupta et al. (1990). Revenaugh (1995, 1999, 2000) applied a Kirchhoff migration approach to back-project P coda recorded in southern California to image lateral variations in scattering intensity within the crust and identified correlations between scattering strength and the locations of faults and other tectonic features. Frederiksen and Revenaugh (2004) applied Born scattering theory to teleseismic P coda to invert for variations in scattering strength near faults in southern California.

Neele and Snieder (1991) used the NARS and GRF arrays in Europe to study long-period teleseismic P coda and found it to be coherent with energy arriving from the source azimuth. They concluded that long-period P coda does not contain a significant amount of scattered energy and can be explained with spherically symmetrical models and is particularly sensitive to structure in upper-mantle low-velocity zones. Ritter et al. (1997, 1998) studied the frequency dependence of teleseismic P coda recorded in the French Massif Central, which they modeled as a 70 km thick layer with velocity fluctuations of 3–7% and heterogeneity scale lengths of 1–16 km. Rothert and Ritter (2000) studied P coda in intermediate-depth Hindu Kush earthquakes recorded at the GRF array in Germany about 44° away. They applied a method based on the theory of Shapiro and Kneig (1993) and Shapiro et al. (1996) and found that the observed wavefield fluctuations are consistent with random crustal heterogeneities of 3–7% and isotropic correlation lengths of 0.6–4.8 km. Ritter and Rothert (2000) used a similar approach on teleseismic P coda to infer differences in scattering strength beneath two local networks in Europe. Hock et al. (2000, 2004) used teleseismic P coda to characterize random lithospheric heterogeneities across Europe using the EFM. They obtained a range of different scale lengths and RMS velocity fluctuations on the order to 3–8%. Nishimura et al. (2002) analyzed transverse components in teleseismic P coda for stations in the western Pacific and noted stronger scattering for stations close to plate boundaries compared to those on stable continents.

In some cases, analysis of P coda can reveal individual scatterers and/or discontinuities at midmantle depths below subduction zone earthquakes (Castle and Creager, 1999; Kaneshima, 2003, 2009; Kaneshima and Helffrich, 1998, 1999, 2003, 2009, 2010; Krüger et al., 2001; Niu and Kawakatsu, 1994, 1997). Other individual scatterers (or regions of strong scattering) have been observed near the CMB from PcP precursors (Brana and Helffrich, 2004; Scherbaum et al., 1997; Weber and Davis, 1990; Weber and Kornig, 1990) and PKP precursors (Thomas et al., 1999; Vidale and Hedlin, 1998).

Shearer and Earle (2004) attempted to systematically characterize and model globally averaged short-period teleseismic P coda from both shallow and deep earthquakes. This was the first attempt to fit a global data set of P-wave amplitudes and coda energy levels with a comprehensive energy-preserving model that specified scattering and intrinsic attenuation throughout the Earth. Examining global seismic network (GSN) data between 1990 and 1999 at source–receiver distances between 10° and 100°, they identified high signal-to-noise records and stacked over 7500 traces from shallow

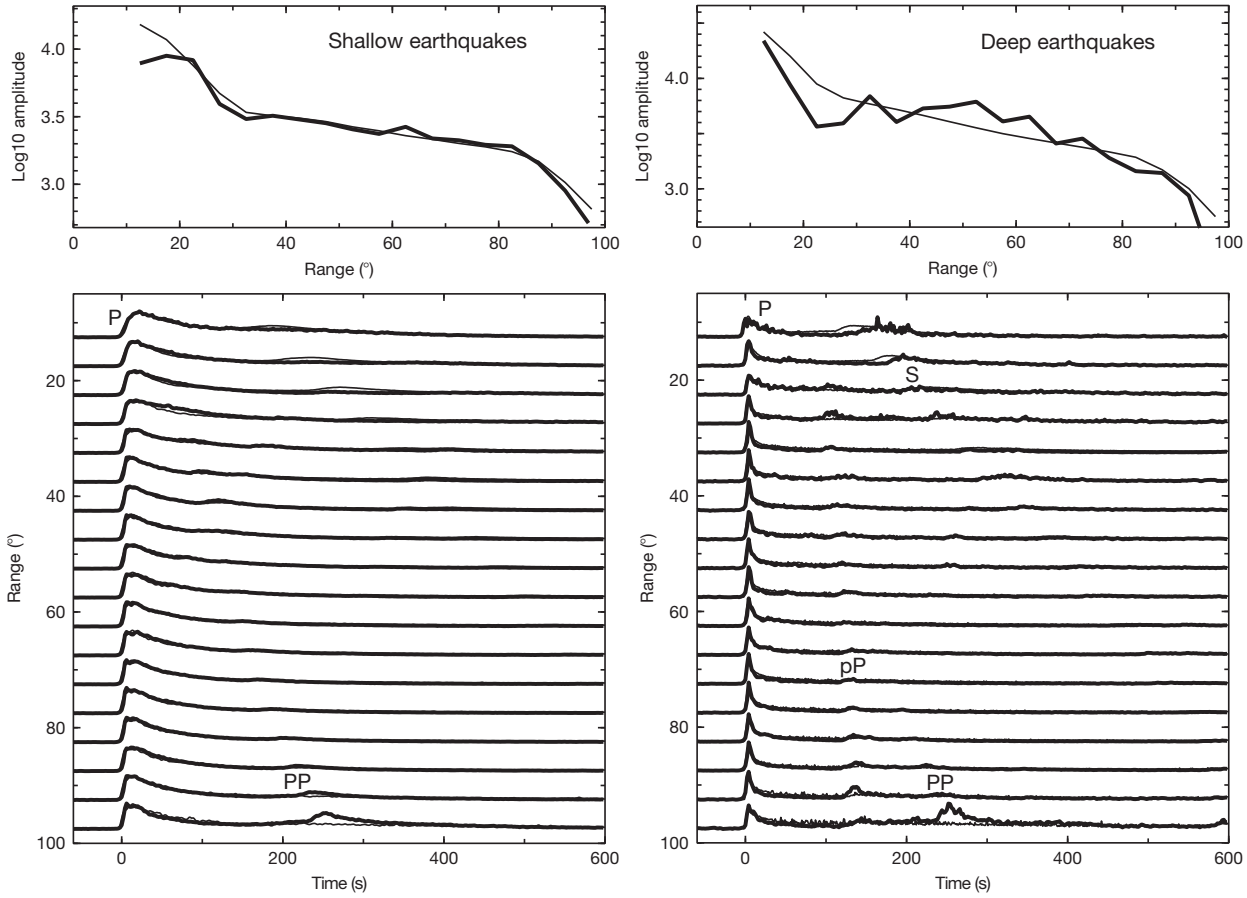

Figure 6 Comparisons between envelope function stacks of teleseismic P-wave arrivals (solid lines) with predictions of a Monte Carlo simulation for a whole-Earth scattering model (thin lines) as obtained by Shearer and Earle (2004). The left panels show results for shallow earthquakes ($\leq$50 km); the right panels are for deep earthquakes ($\geq$400 km). The top panels show peak P-wave amplitude versus epicentral distance. The bottom panels show coda envelopes in 5° distance bins plotted as a function of time from the direct P arrivals, with amplitudes normalized to the same energy in the first 30 s.

events (depth $\leq$ 50 km) and over 650 traces from deep events (depth $\geq$400 km). The stacking method involved summing envelope functions from 0.5 to 2.5 Hz band-pass-filtered traces, normalized to the maximum P amplitude. Peak P amplitudes were separately processed so that absolute P amplitude versus source–receiver distance information was preserved. The coda shape was markedly different between the shallow and deep-event stacks (see **Figure 6**). The shallow earthquake coda was much more energetic and long-lasting than the deep-event coda, indicating that the bulk of the teleseismic P coda from shallow events is caused by near-source scattering above 600 km depth.

Shearer and Earle modeled these observations using a Monte Carlo, particle-based approach (see above) in which millions of seismic phonons are randomly sprayed from the source and tracked through the Earth. They found that most scattering occurs in the lithosphere and upper mantle, as previous results had indicated, but that some lower-mantle scattering was also required to achieve the best fits to the data. Their preferred exponential autocorrelation random heterogeneity model contained 4% RMS velocity heterogeneity at 4 km scale length from the surface to 200 km depth, 3% heterogeneity at 4 km scale between 200 and 600 km, and 0.5% heterogeneity at 8 km scale length between 600 km and the CMB. They assumed equal and correlated P and S fractional velocity perturbations and a density/velocity scaling ratio of 0.8. Intrinsic attenuation was ${}^{\alpha}Q_{\mathrm{I}} = 450$ above 200 km and ${}^{\alpha}Q_{\mathrm{I}} = 2500$ below 200 km, with ${}^{\beta}Q_{\mathrm{I}} = (4/9)\ {}^{\alpha}Q_{\mathrm{I}}$ (an approximation that assumes all the attenuation is in shear). This model produced a reasonable overall fit, for both the shallow and deep-event observations, of the amplitude decay with epicentral distance of the peak P amplitude and the P coda amplitude and duration (see **Figure 6**). These numbers imply that for both P and S waves, the seismic albedo, B_0, is about 75–90% in the upper mantle above 600 km and about 25–35% in the lower mantle, consistent with the total attenuation being dominated by scattering in the upper mantle and by intrinsic energy loss in the lower mantle.

The 4% velocity perturbations for the uppermost layer in the Shearer and Earle (2004) model are in rough agreement with previous P coda analyses by Frankel and Clayton (1986), Flatté and Wu (1988), and Korn (1988); and the S-wave mean

free path of 50 km for the upper 200 km is within the range of mean free paths estimated from regional measurements of lithospheric scattering. However, limitations of the Shearer and Earle (2004) study include the restriction to single-station, vertical-component data (i.e., wave polarization, slowness, and azimuth constraints from three-component and/or array analyses are not used) and a single frequency band near 1 Hz. In addition, the ray theoretical approach cannot properly account for body-to-surface-wave-converted energy, which some array studies suggest are an important component of P coda. In addition, the Shearer and Earle (2004) models are for globally averaged P coda stacks. Later, Shearer and Earle (2008) showed that separating P coda stacks by source and receiver locations reveals significant variations, indicating lateral variations in scattering strength.

Resolving possible lower-mantle scattering using P coda is difficult because of the much stronger scattering from shallow structure. However, Shearer and Earle (2004) found that ~0.5% RMS velocity heterogeneity in the lower mantle was required to achieve the best fit to P coda amplitudes at epicentral distances beyond 50°. This value is substantially more than the estimates for lower-mantle velocity perturbations derived from PKP precursors of 0.1–0.2% from Margerin and Nolet (2003b) and 0.1% from Mancinelli and Shearer (2013).

1.24.3.3 P_n Coda

A prominent feature of long-range records of nuclear explosions across Eurasia is P_n and its coda, which can be observed to distances of more than 3000 km (e.g., Morozov et al., 1998; Ryberg et al., 1995, 2000). As discussed by Nielsen and Thybo (2003), there are two main models for upper-mantle structure that have been proposed to explain these observations: (1) Ryberg et al. (1995, 2000) and Tittgemeyer et al. (1996) proposed random velocity fluctuations between the Moho and about 140 km depth in which the vertical correlation length (0.5 km) is much smaller than the horizontal correlation length (20 km). These fluctuations cause multiple scattering that form a waveguide that can propagate high-frequency P_n to long distances. (2) Morozov et al. (1998), Morozov and Smithson (2000), Nielsen et al. (2003b), and Nielsen and Thybo (2006) favored a model in which P_n is a whispering gallery phase traveling as multiple underside reflections off the Moho, with the coda generated by crustal scattering. Nielsen and Thybo's (2003) preferred model has random crustal velocity perturbations between 15 and 40 km depth with a vertical correlation length of 0.6 km and a horizontal correlation length of 2.4 km. However, Nielsen et al. (2003a) found that the scattered arrivals seen at 800–1400 km distance for profile 'Kraton' required scattering within a layer between about 100 and 185 km depth and could be modeled with 2D finite-difference synthetics assuming 2% RMS velocity variations.

An important aspect of all these models is that their random velocity perturbations are horizontally elongated (i.e., anisotropic). At least for the lower crust, there is also some evidence for this from reflection seismic profiles (e.g., Holliger and Levander, 1992; Wenzel et al., 1987). This contrasts with most modeling of S and P coda, which typically assumes isotropic random heterogeneity.

1.24.3.4 P_{diff} Coda

Another phase particularly sensitive to deep-Earth scattering is P_{diff} and its coda. P_{diff} contains P energy diffracted around the CMB and is observed at distances >98°. The direct phase is seen most clearly at long periods, but high-frequency (~1 Hz) P_{diff} and its coda can be detected to beyond 130° (e.g., Earle and Shearer, 2001). P_{diff} coda is a typically emergent wave train that decays slowly enough that it can commonly be observed for several minutes until it is obscured by the PP and PKP arrivals. Husebye and Madariaga (1970) concluded that P_{diff} coda (which they termed P(diff) tail) could not be explained as simple P diffraction at the CMB or by reflections from the core and suggested that it originated from reflections or multiple paths in the upper mantle (similar to the proposed explanation for PP precursors given by Bolt et al., 1968). However, later work has shown this to be unlikely, given the large differences seen between observations of deep-turning direct P coda and P_{diff} coda. Bataille et al. (1990) reviewed previous studies of P_{diff} coda and suggested that it is caused by multiple scattering near the CMB, with propagation to long distances possibly enhanced by the presence of a low-velocity layer within D″.

Tono and Yomogida (1996) examined P_{diff} coda in 15 short-period records from deep earthquakes at distances of 103°–120° and found considerable variation in the appearance and duration of P_{diff} coda. Comparisons between P_{diff} and direct P waves at shorter distances, as well as particle motion analysis of P_{diff} coda, indicated that the coda was caused by deep-Earth scattering. Tono and Yomogida computed synthetics using the boundary integral method of Benites et al. (1992), applied to a simplified model of an incident wave grazing an irregular CMB. They were able to fit a subset of their observations in which the P_{diff} coda duration was relatively short (<50 s), with bumps on the CMB with minimum heights of 5–40 km. Such large CMB topography is unrealistic given PcP studies, which have indicated a relatively flat and smooth CMB (e.g., Kampfmann and Muüller, 1989; Vidale and Benz, 1992), and PKKP precursor observations that limit CMB RMS topography to <315 m at 10 km wavelength (Earle and Shearer, 1997, see in the succeeding text), but it is likely that volumetric heterogeneity within *D*″ could produce similar scattering. Although the Tono and Yomogida (1996) model included multiple scattering, they could not fit the long tail (>50 s) of some of their P_{diff} observations, and they suggested that for such cases, a low-velocity zone just above the CMB is channeling the scattered energy. Strong heterogeneity and low-velocity zones of varying thicknesses have been observed above the CMB (e.g., see review by Garnero, 2000, and Lay, this volume), but it is not yet clear if these models can explain P_{diff} observations.

Bataille and Lund (1996) argued for a deep origin for P_{diff} coda by comparing coda shapes for P near 90° range and P_{diff} at 102°–105°. The P_{diff} coda is more emergent and lasts much longer than the direct P coda. This argues against a shallow source for the coda because this would produce roughly the same effect on both P and P_{diff}. Baitaille and Lund found that their observed coda decay rate for a single P_{diff} observation at 116° could be fitted with a model of multiple scattering within a 2D shell at the CMB. Tono and Yomogida (1997) examined P_{diff} in records of the 1994 Bolivian deep earthquake at

epicentral distances of 100°–122°. They analyzed both global broadband stations and short-period network stations from New Zealand. They found that short-period energy continued to arrive for over 100 s after P_{diff} itself, more than twice as long as the estimated source duration of the mainshock. Comparisons between the coda decay rate of P_{diff} with other phases, as well as polarization analysis, indicated a deep origin for P_{diff} coda.

Earle and Shearer (2001) stacked 924 high-quality, short-period seismograms from shallow events at source–receiver distances between 92.5° and 132.5° to obtain average P and P_{diff} coda shapes. The results confirm the Bataille and Lund (1996) observation that P coda changes in character near 100°. In particular, P_{diff} becomes increasingly extended and emergent at longer distances. Its peak amplitude also diminishes with increasing distance, but P_{diff} can still be observed in the stacks at 130°. Earle and Shearer also performed a polarization stack (Earle, 1999), which showed that the polarization of P_{diff} coda is similar to P_{diff} (see **Figure 7**). To model these results, Earle and Shearer (2001) applied single-scattering theory for

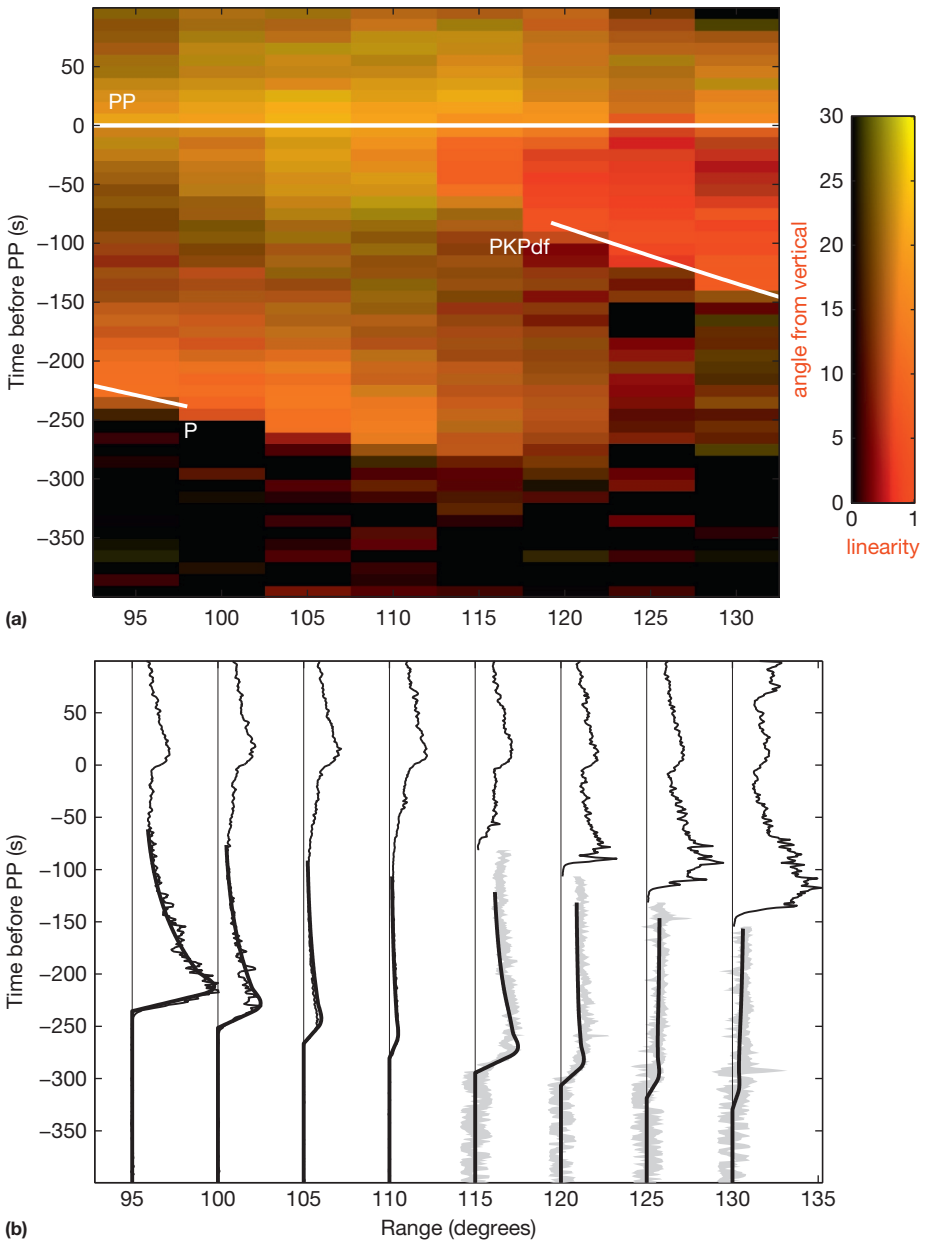

Figure 7 Global seismogram stacks and scattering model predictions for high-frequency P_{diff} from Earle and Shearer (2001). (a) A stacked image of P_{diff} polarization and linearity. Times are relative to the theoretical PP arrival times, and direct P and PKP(DF) are also shown. (b) An amplitude stack of P_{diff} envelopes (wiggly lines) compared to model predictions (smooth lines) for a uniform mantle scattering model. Amplitudes are normalized to the maximum PP amplitude. To better show the small-amplitude P_{diff} arrivals, the traces are magnified by 10 for times 20 s before PKP at distances $>112.5°$. The width of the magnified data traces is equal to the two-sigma error in the data stack, estimated using a bootstrap method.

evenly distributed scatterers throughout the mantle. The resulting synthetics included P-to-P, P_{diff}-to-P, and P-to-P_{diff} scattering paths. They applied a hybrid scheme that used reflectivity to compute deep-turning P and P_{diff} amplitudes and ray theory for the shallower turning rays. Scattering was computed assuming a random medium model with an exponential ACF. Synthetics generated for a scale length of 2 km and 1% RMS velocity variations achieved a good fit to the amplitude and shape of P and P_{diff} coda and a reasonable fit to the polarization angles. Thus, a fairly modest level of whole-mantle scattering appears sufficient to explain the main features in P_{diff} observations, although Earle and Shearer could not exclude the possibility that multiple-scattering models could achieve similar fits. More recently, Rost et al. (2006) stacked short-period seismograms from the GSNs and noticed that almost no short-period P_{diff} is detectable at distances larger than 108°. They suggested that this abrupt disappearance of high-frequency P_{diff} is caused by strong heterogeneity and scattering at the CMB.

1.24.3.5 PP and P′P′ Precursors

The decay in short-period coda amplitude with time following direct P and P_{diff} stops and amplitudes begin to increase some time before the surface-reflected PP phase at distances less than about 110° (at longer distances PKP intercedes). This energy is typically incoherent but sometimes forms distinct arrivals; both are termed PP precursors. Early explanations for PP precursor observations involved topside and bottomside reflections off discontinuities in the upper mantle (Bolt, 1970; Bolt et al., 1968; Gutowski and Kanasewich, 1974; Husebye and Madariaga, 1970; Nguyen-Hai, 1963). It is now recognized that such arrivals do exist and form globally coherent seismic phases that can readily be observed at long periods (e.g., Shearer, 1990, 1991). In particular, the 410 and 660 km discontinuities create discrete topside reflections that follow direct P by about 1.5–2.5 min and underside reflections that proceed PP by similar time offsets. However, the high-frequency PP precursor wavefield is much more continuous, and it is difficult to identify discrete arrivals from upper-mantle discontinuities, although Wajeman (1988) was able to identify underside P reflections from discontinuities at 300 and 670 km depth by stacking broadband data from the NARS array in Europe. Wright and Muirhead (1969) and Wright (1972) used array studies to show that PP precursors often have slownesses that are significantly less than or greater than that expected for underside reflections beneath the PP bouncepoint, which is consistent with asymmetrical reflections at distances near 20° from either the source or the receiver. However, this explanation does not explain the generally continuous nature of the PP precursor wavefield. The currently accepted explanation for the bulk of the PP precursor energy involves scattering from the near-surface and was first proposed by Cleary et al. (1975) and King et al. (1975). Cleary et al. (1975) proposed that PP precursors result from scattering by heterogeneities within and near the crust, as evidenced by travel-time and slowness observations of two Novaya Zemlya explosions recorded by the Warramunga array in Australia. King et al. (1975) modeled PP precursor observations from the Warramunga array and NORSAR using Born single-scattering theory. They assumed 1% RMS variations in elastic properties and a Gaussian autocorrelation model with a 12 km scale length within the uppermost 100 km of the crust and upper mantle. This model successfully predicted the onset times, duration, and slowness of the observed PP precursors but underpredicted the precursor amplitudes, suggesting that stronger scattering, perhaps too large for single-scattering theory, would be required to fully explain the observations. King et al. noted that the focusing of energy at 20° distance by the mantle transition zone could explain the high and low slowness observations of their study and of Wright (1972).

More recently, Rost et al. (2008) studied PP precursors recorded by the Yellowknife array in Canada and used both slowness, back azimuth, and travel-time information to locate mantle scatterers between the surface and about 1000 km depth. Scattering locations below Tonga and the Marianas are consistent with the positions of subducted slabs and the presence of small-scale velocity contrasts from the chemically distinct old oceanic crust penetrating well below 660 km depth.

A related discussion has concerned precursors to PKPPKP (or P′P′), for which the main phase also has an underside reflection near the midpoint between source and receiver. In this case, however, short-period reflections from the 410 and 660 km discontinuities are much easier to observe, and this has become one of the best constraints on the sharpness of these features (e.g., Benz and Vidale, 1993; Davis et al., 1989; Engdahl and Flinn, 1969; Richards, 1972; Xu et al., 2003). However, these reflections arrive 90–150 s before P′P′ and cannot explain the later parts of the precursor wave train. Whitcomb (1973) suggested they were asymmetrical reflections at sloping interfaces, a mechanism similar to that proposed by Wright and Muirhead (1969) and Wright (1972) for PP precursors. King and Cleary (1974) proposed that near-surface scattering near the P′P′ bouncepoint could explain the extended duration and emergent nature of P′P′ precursors. Vinnik (1981) used single-scattering theory to model globally averaged P′P′ precursor amplitudes at three different time intervals and obtained a good fit with a Gaussian ACF of 13 km scale length with RMS velocity perturbations in the lithosphere of about 1.6%.

More recently, Tkalčić et al. (2006) observed P′P′ precursors at epicentral distances $< 10°$, which they interpret as backscattering from small-scale heterogeneities at 150–220 km depth beneath the P′P′ bouncepoints because array studies show that the precursors have the same slowness as the direct phase. Earle et al. (2011) reported and studied P′P′ precursors at 1 Hz between 30° and 50° epicentral distance. Beamforming of data from the LASA array in Montana showed that the arrivals likely result from off-azimuth scattering of PKPbc to PKPbc in the crust and upper mantle. The Earle et al. LASA observations can be approximately fitted with scattering confined to the uppermost 200 km of the crust and mantle, but the scattering geometry should in principle be able to place bounds on scattering strength throughout the entire depth range of the mantle and thus provide a useful complement to PKP precursor studies, which are sensitive only to the lowermost mantle. Wu et al. (2012) also studied high-frequency P′P′ precursors, both using global seismic stations and the Yellowknife and Warramunga arrays, obtaining results that supported the Earle et al. (2011) model of asymmetrical scattering as being the main cause of the precursor energy.

1.24.3.6 PKP Precursors

Perhaps the most direct evidence for deep-Earth scattering comes from observations of precursors to the core phase PKP. They were first noted by Gutenberg and Richter (1934). The precursors are seen at source–receiver distances between about 120° and 145° and precede PKP by up to ~20 s. They are observed most readily at high frequencies and are usually emergent in character and stronger at longer distances. Older, and now discredited, hypotheses for their origin include refraction in the inner core (Gutenberg, 1957), diffraction of PKP from the CMB (Bullen and Burke-Gaffney, 1958; Doornbos and Husebye, 1972), and refraction or reflection of PKP at transition layers between the inner and outer cores (Bolt, 1962; Sacks and Saa, 1969). However, it is now understood that PKP precursors are not caused by radially symmetrical structures but result from scattering from small-scale heterogeneity at the CMB or within the lowermost mantle (Cleary and Haddon, 1972; Haddon, 1972). This scattering diverts energy from the primary PKP ray paths, permitting waves from the AB and BC branches to arrive at shorter source–receiver distances than the B caustic near 145° and earlier than the direct PKP(DF) phase. It should be noted that although the PKP precursors arrive in front of PKP(DF), they result from scattering from different PKP branches. Scattered energy from PKP(DF) itself contributes only to the coda following PKP(DF), not to the precursor wavefield. In addition, the scattering region must be deep to create the precursors. Scattering of PKP(BC) from the shallow mantle will not produce precursors at the observed times and distances. Thus, deep-Earth scattering can be observed uncontaminated by the stronger scattering that occurs in the crust and upper mantle. This unique ray geometry, which results from the velocity drop between the mantle and the outer core, makes PKP precursors invaluable for characterizing small-scale heterogeneity near the CMB.

The interpretation of PKP precursors in terms of scattering was first detailed by Haddon (1972) and Cleary and Haddon (1972). The primary evidence in favor of this model is the good agreement between the observed and theoretical onset times of the precursor wave train for scattering at the CMB. However, analyses from seismic arrays (e.g., Davies and Husebye, 1972; Doornbos, 1976; Doornbos and Husebye, 1972; Doornbos and Vlaar, 1973; Husebye et al., 1976; King et al., 1973, 1974) also showed that the travel times and incidence angles of the precursors were consistent with the scattering theory. Haddon and Cleary (1974) used Chernov scattering theory to show that the precursor amplitudes could be explained with 1% random velocity heterogeneity with a correlation length of 30 km in a 200 km thick layer in the lowermost mantle just above the CMB. In contrast, Doornbos and Vlaar (1973) and Doornbos (1976) argued that the scattering region extends to 600–900 km above the CMB and calculated (using the Knopoff and Hudson, 1964, single-scattering theory) that much larger velocity anomalies must be present. Later, however, Doornbos (1978) used perturbation theory to show that short-wavelength CMB topography could also explain the observations (see also Haddon, 1982), as had previously been suggested by Haddon and Cleary (1974). Bataille and Flatté (1988) concluded that their observations of 130 PKP precursor records could be explained equally well by 0.5–1% RMS velocity perturbations in a 200 km thick layer at the base of the mantle or by CMB topography with RMS height of ~300 m (see also Bataille et al., 1990).

One difficulty in comparing results among these older PKP precursor studies is that it is not clear how many of their differences are due to differences in observations (i.e., the selection of precursor waveforms they examine) compared to differences in theory or modeling assumptions. PKP precursor amplitudes are quite variable, and it is likely that studies that focus on the clearest observations will be biased (at least in terms of determining globally averaged Earth properties) by using many records with anomalously large amplitudes. To obtain a clearer global picture of average PKP precursor behavior, Hedlin et al. (1997) stacked envelope functions from 1600 high signal-to-noise PKP waveforms at distances between 118° and 145° (see **Figure 8**). They included all records, regardless of whether precursors could be observed, to avoid biasing their estimates of average precursor amplitudes. In this way, they obtained the first comprehensive image of the precursor wavefield and found that precursor amplitude grows with both distance and time. The growth in average precursor amplitude with time continues steadily until the direct PKP(DF) arrival; no maximum amplitude peak is seen prior to PKP(DF) as had been suggested by Doornbos and Husebye (1972). This is the fundamental observation that led Hedlin et al. (1997) to conclude that scattering is not confined to the immediate vicinity of the CMB but must extend for some distance into the mantle.

Hedlin et al. (1997) and Shearer et al. (1998) modeled these observations using single-scattering theory for a random medium characterized with an exponential ACF. They found that the best overall fit to the observations was provided with ~1% RMS velocity heterogeneity (this value was later found to be erroneously large owing to a programming bug, see below) at 8 km scale length extending throughout the lower mantle, although fits almost as good could be obtained for 4 and 12 km scale lengths. Similar fits could also be achieved with a Gaussian ACF using a slightly lower RMS velocity heterogeneity. To explain the steady increase in precursor amplitude with time, these models contained uniform heterogeneity throughout the lower mantle, and Hedlin et al. (1997) argued that the data require the scattering to extend at least 1000 km above the CMB and that there is no indication for a significant concentration of the scattering near the CMB. This conclusion was supported by Cormier (1999), who tested both isotropic and anisotropic distributions of scale lengths and found that the PKP precursor envelope shapes are consistent with dominantly isotropic 1% fluctuations in P velocity in the 0.05–0.5 km^{-1} wave number band (i.e., 12–120 km wavelengths).

Most modeling of PKP precursors has used single-scattering theory and the Born approximation. The validity of this approximation for mantle scattering was questioned by Hudson and Heritage (1981). However, Doornbos (1988) found similar results from single- versus multiple-scattering theory for CMB topography of several hundred meters (i.e., the amount proposed by Doornbos, 1978, to explain PKP precursor observations), and Cormier (1995) found the Born approximation to be valid for modeling distributed heterogeneity in the D'' region when compared to results from the higher-order theory of Korneev and Johnson (1993a,b). More recently,

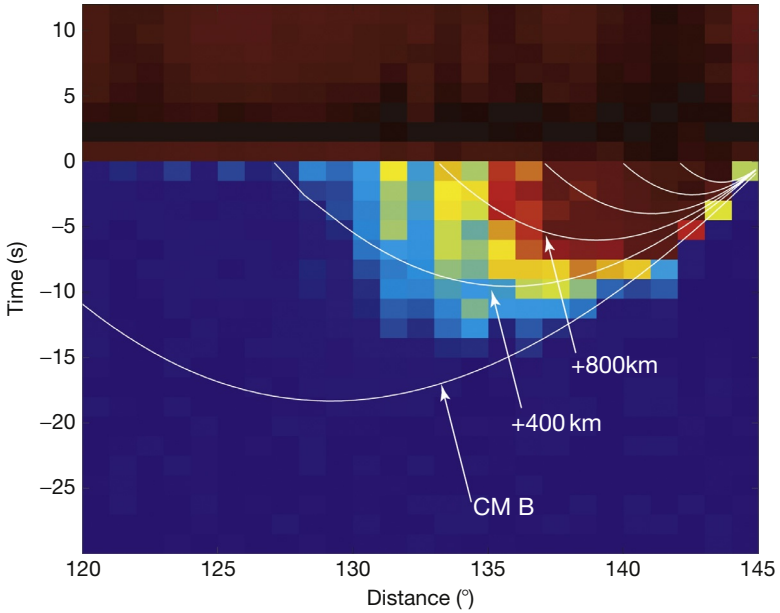

Figure 8 PKP precursors as imaged by stacking 1600 short-period seismograms by Hedlin et al. (1997). The colors indicate the strength of the precursors, ranging from dark blue (zero amplitude) to green, yellow, red, and brown (highest amplitudes). The onset of PKP(DF) is shown by the edge of the brown region at zero time. The precursors exhibit increasing amplitude with both distance and time. The white curves show the theoretical precursor onset times for scattering at 400 km depth intervals above the core–mantle boundary (CMB).

Margerin and Nolet (2003a,b) modeled PKP precursors using radiative transfer theory and a Monte Carlo method (see the preceding text). Their results supported Hedlin et al. (1997) and Shearer et al. (1998) in finding that whole-mantle scattering fit the data better than scattering restricted to near the CMB, but they obtained much smaller P-velocity perturbations of 0.1–0.2% versus the 1% originally proposed by Hedlin et al. The accuracy of the Margerin and Nolet result for the velocity perturbations was recently confirmed by Mancinelli and Shearer (2013), who used a multiple-scattering Monte Carlo method to show that updated PKP precursor stacks could be fit with 0.1% RMS velocity perturbations. They found that similar results could be obtained using Born theory and that the 1% value in the older Hedlin et al. work was due to a programming mistake. Margerin and Nolet showed that the Born approximation is accurate for whole-mantle scattering models only when the velocity heterogeneity is $< 0.5\%$. Finally, they concluded that exponential correlation length models do not fit the distance dependence in PKP precursor amplitudes as well as models containing more small-scale structure.

The steady increase in amplitude with time in PKP precursor stacks requires that globally averaged small-scale mantle heterogeneity extends above the lowermost few hundred kilometers of the mantle. However, determining exactly how far the scattering must extend above the CMB is a challenging problem because only a small fraction of the precursor wavefield is sensitive to scattering above 600 km from the CMB, and this fraction continues to shrink for shallower scattering depths. For example, at 1200 km above the CMB, precursors are produced only between 138° and 145° and arrive at most 3 s before PKP(DF) (see **Figure 8**). Separating the amplitude contribution from these arrivals from that produced by scattering at deeper depths in the mantle is very difficult, particularly when the pulse broadening caused by realistic source-time functions and shallow scattering and reverberations are taken into account. An alternative approach to constraining the strength of midmantle scattering is to examine the scattered PKP wavefield after the direct PKP(DF) arrival (Hedlin and Shearer, 2002). This is comprised of a sum of PKP(DF) coda and scattered PKP(AB) and PKP(BC) energy. In principle, if the contribution from the PKP(DF) coda could be removed, the remaining scattered wavefield would provide improved constraints on the strength of midmantle scattering. However, Hedlin and Shearer (2002) found that this approach did not provide improved depth resolution of mantle scattering compared to previous analyses of PKP precursors, owing at least in part to relatively large scatter in coda amplitudes as constrained by a data resampling analysis. Their results were, however, consistent with uniform mantle scattering with 1% RMS random velocity perturbations at 8 km scale length.

The preceding discussion considered only average PKP precursor properties and models with radial variations in scattering. However, PKP precursor amplitudes are quite variable, as noted by Bataille and Flatté (1988) and Bataille et al. (1990), suggesting lateral variations in scattering strength. Vidale and Hedlin (1998) identified anomalously strong PKP precursors for ray paths that indicated intense scattering at the CMB beneath Tonga. Wen and Helmberger (1998) observed broadband PKP precursors from near the same region, which they modeled as Gaussian-shaped ultra-low-velocity zones of 60–80 km height with P-velocity drops of 7% or more over 100–300 km (to account for the long-period part of the precursors), superimposed on smaller-scale anomalies to explain the high-frequency part of the precursors.

Array analyses can resolve the source–receiver ambiguity of PKP scattering and often permit location of individual

scatterers or regions of strong scattering in the lower mantle. Thomas et al. (1999) used German network and array records of PKP precursors to identify isolated scatterers in the lower mantle. Niu and Wen (2001) identified strong PKP precursors for South American earthquakes recorded by the Jarray in Japan, which they modeled with 6% velocity perturbations within a 100 km thick layer just above the CMB in a 200 km by 300 km area west of Mexico. Cao and Romanowicz (2007) used Canadian Yellowknife array records of an earthquake doublet to identify receiver-side scatterers at depths ranging from 0 to 600 km above the CMB and scattering angles between 16° and 46°. They found that the scatterer locations suggest they may be fragments of fossil slabs from ancient subduction under North America. Miller and Niu (2008) used data from Caribbean arrays to image strong scatterers near the CMB, which are surrounded by high-velocity anomalies associated with the Farallon slab, and suggested a segregation mechanism that could concentrate the scatterers into a localized region. Thomas et al. (2009) examined South Pacific earthquakes recorded by German and Ethiopian arrays and studied both PKP precursors (seen for both arrays) and the amplitude of diffractions from the PKP b caustic (anomalously large for the Ethiopian data). They found that low-velocity regions just above the CMB could act as waveguides to produce large PKP b-diffractions but that these low-velocity regions must also contain small-scale heterogeneities to explain the high-frequency scattering seen in the data. They proposed that melt inclusions could explain both the lower velocities seen at long wavelengths and produce the scattering observed at short wavelengths.

Hedlin and Shearer (2000) attempted to systematically map lateral variations in scattering strength using a global set of high-quality PKP precursor records. Their analysis was complicated by the limited volume sampled by each source–receiver pair, the ambiguity between source- and receiver-side scattering, and the sparse and uneven data coverage. However, they were able to identify some large-scale variations in scattering strength that were robust with respect to data resampling tests. These include stronger than average scattering beneath Central Africa, parts of North America, and just north of India and weaker than average scattering beneath South and Central America, eastern Europe, and Indonesia.

Finally, it should be noted that the earliest onset time of observed PKP precursors agrees closely with that predicted for scattering at the CMB (e.g., Cleary and Haddon, 1972; Shearer et al., 1998). If scattering existed in the outer core at significant depths below the CMB, this would cause arrivals at earlier times than are seen in the data. This suggests that no observable scattering originates from the outer core, although a quantitative upper limit on small-scale outer-core heterogeneity based on this constraint has not yet been established. Such a limit would be useful to test the recent hypothesis of Dai and Song (2008) that movement of outer-core heterogeneities could explain their observations of increased temporal variability in travel times for core seismic phases compared to mantle phases.

1.24.3.7 PKKP Precursors and $PKKP_X$

PKKP is another seismic core phase that provides information on deep-Earth scattering. Precursors to PKKP have been observed within two different distance intervals. PKKP(DF) precursors at source–receiver distances beyond the B caustic near 125° are analogous to the PKP precursors discussed in the previous section and result from scattering in the mantle. Doornbos (1974) detected these precursors in NORSAR (Norwegian Seismic Array) records of Solomon Islands earthquakes and showed that their observed slownesses were consistent with scattering from the deep mantle. At ranges $<125°$, PKKP(BC) precursors can result from scattering off short-wavelength CMB topography. Chang and Cleary (1978, 1981) observed these precursors from Novaya Zemlya explosions recorded by the LASA array in Montana at about 60° range. These observations were suggestive of CMB topography but had such large amplitudes that they were difficult to fit with realistic models. Doornbos (1980) obtained additional PKKP(BC) precursor observations from NORSAR records from a small number of events at source–receiver distances between 80° and 110°. He modeled these observations with CMB topography of 100–200 m at 10–20 km horizontal scale length. Motivated by PKKP precursor observations (see the succeeding text), Cleary (1981) suggested that some observations of P′P′ precursors (e.g., Adams, 1968; Haddon et al., 1977; Husebye et al., 1977; Whitcomb and Anderson, 1970) might be explained as CMB-scattered PKKKP precursors.

A comprehensive study of PKKP(BC) precursors was performed by Earle and Shearer (1997), who stacked 1856 high-quality PKKP seismograms, obtained from the GSN at distances between 80° and 120°. PKKP is most readily observed at high frequencies (to avoid interference from low-frequency S coda), so the records were band-pass-filtered to between 0.7 and 2.5 Hz. To avoid biasing the stacked amplitudes, no consideration was given to the visibility or lack of visibility of PKKP precursors on individual records. The resulting stacked image showed that energy arrives up to 60 s before direct PKKP(BC) and that average precursor amplitudes gradually increase with time. Earle and Shearer (1997) modeled these observations using Kirchhoff theory for small-scale CMB topography. Their best-fitting model had a horizontal scale length of 8 km and RMS amplitude of 300 m. However, they identified a systematic misfit between the observations and their synthetics in the dependence of precursor amplitude with source–receiver distance. In particular, the Kirchhoff synthetics predict that precursor amplitude should grow with range but this trend is not apparent in the data stack. Thus, the model underpredicts the precursor amplitudes at short ranges and overpredicts the amplitudes at long ranges. Earle and Shearer (1997) and Shearer et al. (1998) explored possible reasons for this discrepancy between PKKP(BC) precursor observations and predictions for CMB topography models. They were not able to identify a very satisfactory explanation but speculated that scattering from near the ICB might be involved because it could produce precursor onsets that agreed with the observations (see Figure 13 from Shearer et al., 1998). However, scattering angles of 90° or more are required and it is not clear, given the expected amplitude of the direct PKKP(DF) phase, that the scattered amplitudes would be large enough to explain the PKKP(BC) precursor observations. They concluded that strong inner-core scattering would be required, which could only be properly modeled with a multiple-scattering theory. Regardless of the possible presence of scattering from

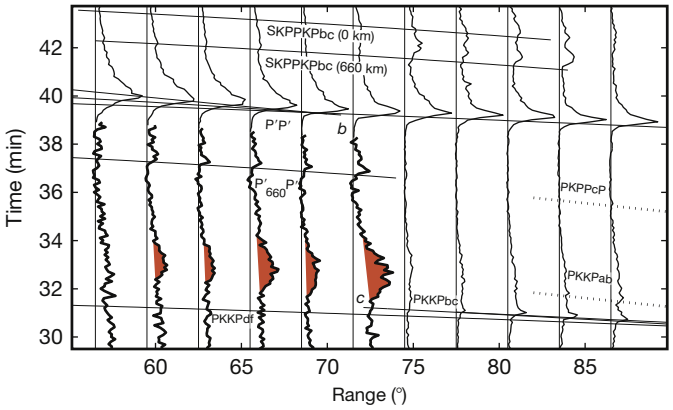

Figure 9 A stack of 994 seismograms from Earle and Shearer (1998), showing the $PKKP_X$ phase (red) in the high-frequency wavefield preceding P′P′. The stacked traces are normalized to the maximum P′P′ amplitude and are plotted with respect to the origin time of a zero depth earthquake. To better show the $PKKP_X$ arrival, amplitudes are magnified by eight for traces preceding P′P′ at epicentral distances $<73°$ (indicated by the heavy lines). Labels indicate observed phases and the position of the P′P′ b and PKKP c caustics.

sources outside the CMB, these PKKP(BC) precursor observations can place upper limits on the size of any CMB topography. Earle and Shearer (1997) concluded that the RMS topography could not exceed 315 m at 10 km wavelength.

Earle and Shearer (1998) stacked global seismograms using P′P′ as a reference phase and identified an emergent, long-duration, high-frequency wave train near PKKP (see **Figure 9**), which they named $PKKP_X$ because it lacked a clear explanation. $PKKP_X$ extends back from the PKKP(C) caustic at 72° to a distance of about 60°. Its 150 s long duration, apparent move-out, and proximity to PKKP suggest a deep scattering origin. However, Earle and Shearer were not able to match these observations with predictions of single-scattering theory for scattering in the lower mantle, CMB, or ICB. They speculated that some form of multiple-scattering model at the CMB might be able to explain the observations, perhaps involving a low-velocity zone just above the CMB to trap high-frequency energy, a model similar to that proposed to explain P_{diff} coda by Bataille et al. (1990), Tono and Yomogida (1996), and Bataille and Lund (1996). Earle (2002) further explored the origin of $PKKP_X$ and other scattered phases near PKKP by performing slant stacks on LASA data. His results suggested that, in addition to off-great-circle-path near-CMB scattering, near-surface P-to-PKP scattering is likely an important contributor to high-frequency energy around PKKP at distances between 50° and at least 116°. In particular, such scattering arrives at the same time as observations of PKKP precursors and $PKKP_X$, thus providing a possible explanation for why PKKP precursor amplitudes are hard to fit purely with CMB scattering models. However, quantitative modeling of P-to-PKP scattering has not yet been performed to test this hypothesis.

More recently, Rost and Earle (2010) examined PKKP precursors using small-aperture seismic arrays in Canada and India. Beamforming analysis showed regions of strong scattering near the CMB beneath the Caribbean, Patagonia, the Antarctic Peninsula, and southern Africa. The 1 Hz scattered energy suggests small-scale chemical heterogeneity, and Rost and Earle speculated that the scattering beneath Antarctica and the Americas is related to ancient subducted crust, whereas the southern Africa scattering may be related to partial melt associated with the edge of a large low shear velocity province just above the CMB in that region.

1.24.3.8 PKiKP and PKP Coda and Inner-Core Scattering

The ICB-reflected phase PKiKP is of relatively low amplitude and observations from single stations are fairly rare, particularly at source–receiver distances $<50°$. However, improved signal-to-noise ratio and more details can be obtained from analysis of short-period array data. Vidale and Earle (2000) examined 16 events at 58°–73° range recorded by the LASA in Montana between 1969 and 1975. As shown in **Figure 9**, a slowness versus time stack of the data (band-pass-filtered at 1 Hz) revealed a 200 s long wave train with an onset time and slowness in agreement with that predicted for PKiKP. They attributed this energy to scattering from the inner core because it arrived at a distinctly different slowness from late-arriving P coda and it was much more extended in time than LASA PcP records for the same events. The PKiKP wave train takes 50 s to reach its peak amplitude and averages only about 2% of the amplitude of PcP. Direct PKiKP is barely visible, with an amplitude close to its expected value, which is small because the ICB reflection coefficient has a node at distances near 72° (e.g., Shearer and Masters, 1990).

Vidale and Earle (2000) fitted their observations with synthetics computed using single-scattering theory applied to a model of random inner-core heterogeneity with 1.2% RMS variations in density and the Lamé parameters (λ and μ) and a correlation distance of 2 km, assuming an exponential autocorrelation model. They assumed ${}^{\alpha}Q_I = 360$ uniformly throughout the inner core, a value obtained from a study (Bhattacharyya et al., 1993) of pulse broadening of PKP(DF) compared to PKP(BC). They noted that without inner-core attenuation, the predicted scattered PKiKP wave train would take 100 s to attain its peak value and would last 350 s. The low value of ${}^{\alpha}Q_I$ resulted in only the shallow penetrating P waves retaining sufficient amplitude to be seen. Model-predicted scattering angles were near 90°, making the scattering most sensitive to variations in inner-core λ. Vidale and Earle (2000) found a trade-off between the various free parameters

in their model and picked their 2 km correlation length because it minimized the required RMS variation of 1.2% necessary to fit the observations. They computed a fractional energy loss of 10% from scattering in the top 300 km of the inner core, helping to justify the use of the Born single-scattering approximation. Vidale et al. (2000) examined LASA data for two nuclear explosions 3 years apart and separated by <1 km. They identified systematic time shifts in PKiKP coda, which they explained as resulting from differential inner-core rotation, as previously proposed by Song and Richards (1996). In contrast, much smaller time differences are observed in PKKP and PKPPKP arrivals, supporting the idea that the time dependence originates in the inner core. Vidale et al. (2000) estimated an inner-core rotation rate of 0.15° per year.

Cormier et al. (1998) measured pulse broadening in PKP(DF) waveforms and showed that they could be fitted either with intrinsic inner-core attenuation or with scattering caused by random layering (1D) with 8% P-velocity perturbations and 1.2 km scale length. Cormier and Li (2002) inverted 262 broadband PKP(DF) waveforms for a model of inner-core scattering attenuation based on the dynamic composite elastic medium theory of Kaelin and Johnson (1998) for a random distribution of spherical inclusions. They not only obtained a mean velocity perturbation of ~8% and a heterogeneity scale length of ~10 km but also observed path-dependent differences in these parameters, with both depth dependence and anisotropy in the size of the scattering attenuation. They suggested that scattering attenuation is the dominant mechanism of attenuation in the inner core in the 0.02–2 Hz frequency band. Cormier and Li (2002) argued that the large discrepancy in RMS velocity perturbation and scale length between their study (RMS = 8%, scale length = 10 km) and the model (RMS = 1.2%, scale length = 2 km) of Vidale and Earle (2002) may be due to the significant intrinsic attenuation assumed by Vidale and Earle and differences in depth sensitivity between the studies.

Poupinet and Kennett (2004) analyzed PKiKP recorded by Australian broadband stations and the Warramunga array for events at short distances ($<\sim45°$). They found that PKiKP could frequently be observed on single traces filtered at 1–5 Hz. In contrast to Vidale and Earle (2000), they found that PKiKP typically had an impulsive onset with a coda that decayed rapidly to a relatively small amplitude that persisted for more than 200 s. Although most of the Poupinet and Kennett results were for shorter source–receiver distances than the 58°–73° range of the Vidale and Earle study, they did analyze one event at 74° that exhibited similar behavior. Poupinet and Kennett suggested that the differences in the appearance of PKiKP coda between the studies may reflect different sampling latitudes at the ICB and different frequency filtering. They pointed to similarities in the appearance of PKiKP coda and P_{diff} coda (see the preceding text) and speculated that both result from their interaction with a major interface that may involve energy channeling to produce an extended wave train. Poupinet and Kennett (2004) argued that the high-frequency nature of PKiKP coda excludes an origin deep within the inner core where attenuation is high and suggested that multiple scattering near the ICB is a more likely mechanism.

Koper et al. (2004) analyzed PKiKP coda waves recorded by short-period seismic arrays of the International Monitoring System (IMS) at source–receiver distances ranging from 10° to 90°. Stacked beam envelopes for the 10°–50° data showed impulsive onsets for PcP, ScP, and PKiKP, but a markedly different coda for PKiKP, which maintained a nearly constant value that lasted for over 200 s. This is consistent with the Poupinet and Kennett (2004) results at similar distances and supports the idea that inner-core scattering is contributing to the PKiKP coda. At distances from 50° to 90°, Koper et al. (2004) found one event at 56° with a PKiKP coda that increased in amplitude with time, peaking nearly 50 s after the arrival of direct PKiKP, behavior very similar to the LASA observations of Vidale and Earle (2000). At 4 Hz, 13 out of 36 PKiKP observations had emergent codas that peaked at least 10 s into the wave train. However, more commonly, the peak coda amplitude occurred at the onset of PKiKP. Koper et al. (2004) found that the average PKiKP coda decay rate was roughly constant between stacks at short- and long-distance intervals, supporting the hypothesis of inner-core scattering. They argued that the best distance range to study inner-core scattering is 50°–75°, where the direct PKiKP amplitude is weak (because of a very small ICB reflection coefficient) so that scattering from the crust and mantle is unlikely to contribute as much to the observed coda as scattering from the inner core. However, they also discussed the possibility that CMB scattering could deflect a P wave into a PKiKP wave that could reflect from the ICB at an angle with a much higher reflection coefficient and contribute to the observed coda.

Leyton and Koper (2007a,b) applied single-scattering theory to model PKiKP coda observations and found that the emergent coda seen in previous observations (e.g., **Figure 10**) can only be produced by scattering in the uppermost 350 km of the inner core. They obtained an average Q_C of 500 for the inner core, but with a geographic dependence in which most PKiKP coda observations are from the Pacific Ocean and Asia and relatively few from the Atlantic. This implies that inner-core scattering has a hemispheric dependence, which has also been observed in other properties (e.g., anisotropy strength) of the outermost inner core. Peng et al. (2008) presented additional LASA records of PKiKP coda, which they forward modeled using the Monte Carlo seismic phonon code of Shearer and Earle (2004). Consistent with Leyton and Koper (2007a), they found that the general properties of the PKiKP coda could be explained with small-scale volumetric heterogeneities in the uppermost few hundred kilometers of the inner core. Cormier (2007) modeled both backscattered PKiKP and forward-scattering PKP(DF) waves at frequencies up to 1 Hz using a 2D pseudospectral finite-difference code and showed how an anisotropic texture with hemispheric variations could explain the observations. Cormier et al. (2011) further developed this model and related it to hypotheses for inner-core crystal growth. Calvet and Margerin (2008) proposed a model in which uppermost inner-core scattering and attenuation are explained with an aggregate of randomly oriented anisotropic blobs of aligned iron crystals.

$PKP(C)_{diff}$ is the P wave that diffracts around the ICB and is seen as an extension of the PKP(BC) branch to distances beyond 153°. Nakanishi (1990) analyzed Japanese records of $PKP(C)_{diff}$ coda from a deep earthquake in Argentina and suggested that scattering near the bottom of the upper mantle could explain its times and slowness. Tanaka (2005) examined $PKP(C)_{diff}$ coda from 28 deep earthquakes recorded using small-aperture short-period seismic arrays of the IMS at epicentral distances of 153°–160°. Beamforming at 1–4 Hz

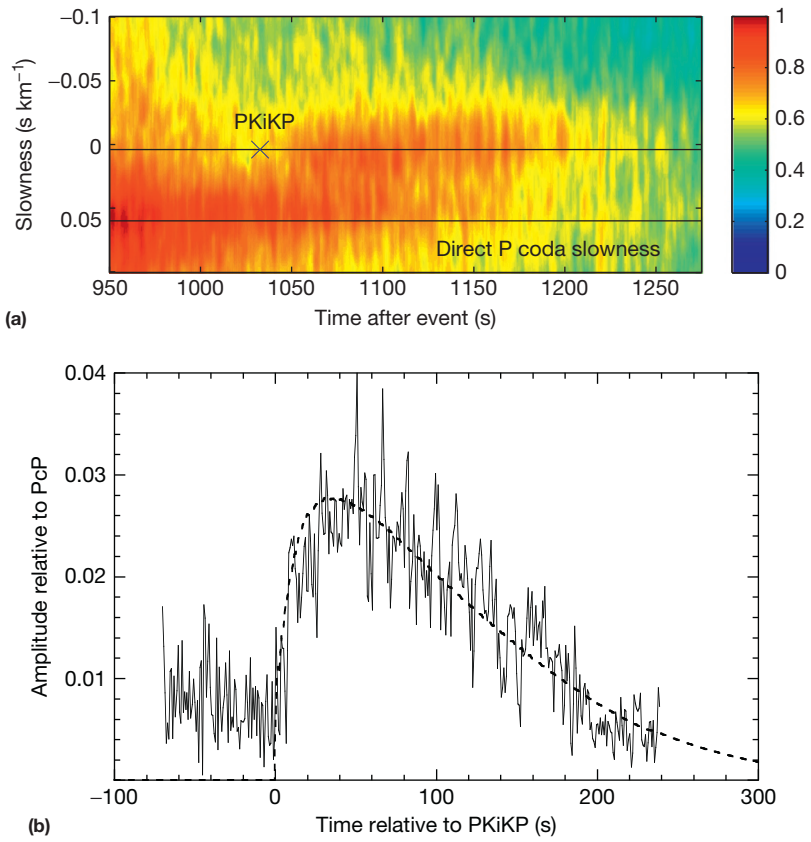

Figure 10 PKiKP coda as observed and modeled by Vidale and Earle (2000) for data from 12 earthquakes and four nuclear explosions recorded at the LASA in Montana. The top panel (Zhi-gang Peng, personal communication) shows a slowness versus time envelope function stack of energy arriving between 950 and 1270 s from the event origin times. The predicted direct PKiKP arrival is shown with the ×. Late P coda forms the stripe seen at a slowness near 0.5 s km^{-1}. PKiKP coda is the stripe seen near zero slowness. The bottom panel compares a PKiKP amplitude stack (wiggly line) to the predicted scattering envelope for an inner-core random heterogeneity model (dashed line).

resolved the slownesses and back azimuths of PKP(DF), PKP(C)$_{diff}$, and PKP(AB). The PKP(C)$_{diff}$ coda lasted longer than PKP(AB), but the wide slowness distribution of PKP(C)$_{diff}$ coda is difficult to explain as originating solely from the ICB, and Tanaka suggested that scattering near the CMB is an important contributor to PKP(C)$_{diff}$ coda.

Vidale and Earle (2005) studied PKP coda from seven Muruoa Island nuclear explosions over a 10-year period recorded by the NORSAR at an epicentral distance of 136°. They observed complicated arrivals lasting ~10 s that were more extended than the relatively simple pulses observed for direct P waves from explosions recorded in the western United States. Vidale and Earle suggested that these complications likely arose from scattering at or near the ICB. They showed that small time shifts in the PKP coda were consistent with shifts predicted for point scatterers in an inner core that rotated at 0.05°–0.1° per year, although they could not entirely rule out systematic changes in source location.

1.24.3.9 Other Phases

Emery et al. (1999) computed the effect of different types of D'' heterogeneity on S_{diff}, using both the Langer and Born approximations. They found that their long-period S_{diff} observations are not particularly sensitive to the types of small-scale heterogeneities proposed to explain other data sets. Cormier (2000) used the coda power between P and PcP and S and ScS, together with limits on pulse broadening in PcP and ScS waveforms, to model D'' heterogeneity using a 2D pseudospectral calculation. He attempted to resolve the heterogeneity power spectrum over a wide range of scale lengths, to bridge the gaps among global tomography studies, D'' studies, and PKP precursor analyses.

Lee et al. (2003) noted an offset in S coda observations for Central Asian earthquakes (150–250 km deep) recorded about 750 km away at station AAK. The offset occurred near the ScS arrivals in coda envelopes at 10 and 15 s period. At shorter periods (1–4 s), a change in coda decay rate appeared associated with the ScS arrival. They simulated these observations with a Monte Carlo method based on radiative transfer theory and isotropic scattering. For a two-layer mantle model (separated at 670 km), their best-fitting synthetics at 4 s had a total scattering coefficient g_0 of about 1.3×10^{-3} km^{-1} and 6.0×10^{-4} km^{-1} for the upper and lower layers, respectively. Corresponding results at 10 s were about 4.7×10^{-4} km^{-1} and 2.6×10^{-4} km^{-1}. Lee et al. (2006) further studied S and ScS coda envelopes from deep earthquakes recorded at nine distributed global seismic stations and modeled the results with a Monte Carlo method with isotropic scattering and obtained estimates of both the frequency and depth dependence of

average mantle scattering. They also identified regions of stronger scattering, including beneath Central Asia and New Guinea, and argued that scattering attenuation is much stronger than intrinsic attenuation in the 4–10 s band for some regions.

1.24.4 Discussion

Scattering from small-scale irregularities has now been detected at all depths inside the Earth with the exception of the fluid outer core, although many details of this heterogeneity (power spectral density, depth dependence, etc.) remain poorly resolved, at least on a global scale. Scattering is the strongest near the surface, but significant scattering also occurs throughout the lower mantle (e.g., Cormier, 1999; Earle and Shearer, 2001; Hedlin et al., 1997; Margerin and Nolet, 2003b; Shearer and Earle, 2004; Shearer et al., 1998). Small-scale heterogeneity within the deep mantle is almost certainly compositional in origin because thermal anomalies would diffuse away over relatively short times (Hedlin et al., 1997; Helffrich and Wood, 2001) and supports models of incomplete mantle mixing (e.g., Allègre and Turcotte, 1986; Gurnis and Davies, 1986; Morgan and Morgan, 1999; Olson et al., 1984). Helffrich and Wood (2001) discussed the implications of small-scale mantle structure in terms of convective mixing models and suggested that the scatterers are most likely remnants of lithospheric slabs. Assuming subduction-induced heterogeneities are 11–16% of the volume of the mantle, they proposed that most of this heterogeneity occurs at scale lengths <4 km, where it would have little effect on typically observed seismic wavelengths. Meibom and Anderson (2003) discussed the implications of small-scale compositional heterogeneity in the upper mantle, where partial melting may also be an important factor.

There is a large gap between the smallest scale lengths resolved in global mantle tomography models and the ~10 km scale length of the random heterogeneity models proposed to explain scattering observations. Chevrot et al. (1998) showed that the amplitude of the heterogeneity in global and regional tomography models obeys a power law decay with wave number, that is, that most of the power is concentrated at low spherical harmonic degree, a result previously noted by Su and Dziewonski (1991) for global models. For the shallow mantle, this is probably caused in part by continent–ocean differences (G. Masters, personal communication, 2005), but a decay of order k^{-2}–k^{-3} is also predicted for heterogeneity caused by temperature variations in a convecting fluid (Cormier, 2000; Hill, 1978). However, this decay cannot be extrapolated to very small scales because it would predict heterogeneity much weaker than what is required to explain seismic scattering observations at ~10 km scale. As discussed by Cormier (2000), the most likely explanation is a change from thermal to compositionally dominated heterogeneity and that small-scale (<100 km) mantle perturbations are chemical in origin. Spherical heterogeneities of radii 38 km or smaller can be entrained in mantle flow, assuming a mantle viscosity of 10^{21} Pa s, a density contrast of 1 g cc^{-1}, and a convective velocity of 1 cm year^{-1} (Cormier, 2000). Because settling rate scales as the radius squared, smaller blobs will be entrained even at much smaller density contrasts.

The role of the core–mantle and ICBs in small-scale scattering is not yet clear. The D'' region has stronger heterogeneity than the midmantle in tomography models, and large velocity contrasts have been identified in specific regions, including ULVZs and strong individual PKP scatterers (e.g., Niu and Wen, 2001; Vidale and Hedlin, 1998; Wen and Helmberger, 1998). However, globally averaged PKP precursor studies do not find evidence for stronger scattering at the CMB than in the rest of the lower mantle (Hedlin et al., 1997; Margerin and Nolet, 2003b). CMB topography can also produce scattering and has been invoked by some authors to explain PKP and PKKP precursors but fails to predict globally averaged PKKP precursor amplitude versus distance behavior (Earle and Shearer, 1997). Vidale and Earle modeled PKiKP coda observations with bulk scattering within the inner core, while Poupinet and Kennett (2004) suggested that scattering from near the ICB, where several recent studies have found evidence for anomalous structures (e.g., Koper and Dombrovskaya, 2005; Krasnoshchekov et al., 2005), was more likely responsible for their PKiKP coda observations. Strong attenuation is observed in the inner core, but it is not yet clear how much of this is caused by intrinsic versus scattering attenuation. Inner-core scattering might be caused by small-scale textural anisotropy (Cormier et al., 1998, 2011; Vidale and Earle, 2000) or by compositionally induced variations in partial melt (Vidale and Earle, 2000).

At shallow depths, it is clear that there are both strong scattering and significant lateral variations in scattering strength, but the number and diversity of studies on lithospheric scattering make it difficult to draw general conclusions. There is a large literature on both the theory of seismic scattering and on coda observations, but there has been much less effort to integrate these studies into a comprehensive picture of scattering throughout Earth's interior. Review articles (e.g., Aki, 1982; Fehler and Sato, 2003; Herraiz and Espinoa, 1987; Matsumoto, 1995; Sato, 1991) and the book by Sato and Fehler (1998, 2012) are certainly helpful, but their summaries often involve comparisons among studies that differ in many key respects, such as their choice of seismic phase (P, S, etc.); their epicentral distance, frequency range, and time window; and their modeling assumptions (e.g., single scattering, MLTW, finite difference, and radiative transfer). It is not always clear whether models proposed to explain one type of data are supported or contradicted by other types of data. For example, models with horizontally elongated crust and/or upper-mantle heterogeneity appear necessary to explain long-range P_n propagation across Eurasia, and many models of lower crustal reflectors are anisotropic (e.g., Holliger and Levander, 1992; Wenzel et al., 1987). Tkalčić et al. (2010) proposed anisotropic scattering from near-receiver random heterogeneity to explain their observations of anticorrelated PcP and PKiKP amplitudes. Yet almost all modeling of local earthquake coda assumes isotropic random heterogeneity.

A promising development is the increasingly open availability at data centers of seismic records from local and regional networks, portable experiments, and the GSNs. This should enable future coda studies to be more comprehensive and analyze larger numbers of stations around the world using a standardized approach. This would help to establish a baseline of globally averaged scattering properties and maps of

lateral variations in scattering strength over large regions. Data from small-aperture seismic arrays are also very important, because they permit beamforming analysis that can pinpoint the locations of individual scatterers or scattering regions, as several recent studies have shown (e.g., Cao and Romanowicz, 2007; Miller and Niu, 2008; Rost and Earle, 2010; Rost et al., 2008; Thomas et al., 2009). Ultimately, more detailed information on lithospheric heterogeneity (amplitude, scale length, and anisotropy) will enable more detailed comparisons to geologic and petrologic constraints on rock chemistry (e.g., Levander et al., 1994; Ritter and Rothert, 2000).

Analyses of deep-Earth scattering have also used a variety of different phase types and modeling approaches. Even today, there are still fundamental features in the high-frequency wavefield, such as $PKKP_X$ (Earle, 2002), that lack definitive explanations and have never been quantitatively modeled. However, given recent improvements in modeling capabilities (e.g., Monte Carlo calculations based on radiative transfer theory and whole Earth finite-difference calculations), there is now a clear path toward creating 1D models of Earth's average scattering properties and resolving between scattering and intrinsic attenuation mechanisms. It appears that a substantial part of seismic attenuation at high frequencies is caused by scattering rather than intrinsic energy loss, but fully resolving trade-offs between Q_{Sc} and Q_I will require analysis of scattering observations at a wide range of frequencies and epicentral distances. An interesting comparison can be made with seismologist's efforts to map bulk seismic velocity variations. Regional velocity profiling of the upper mantle gave way in the 1980s to comprehensive velocity inversions (i.e., 'tomography') to image global 3D mantle structure. This required working with large data sets of body-wave travel-time and surface-wave phase-velocity measurements and developing and evaluating methods to invert large matrices. The earliest models were crude and controversial in their details, but rapid progress was made as different groups began comparing their results. We may be poised to make similar advances in resolving Earth scattering. But progress will require improved sharing of data from local and regional networks as well as greater testing and standardization of numerical simulation codes. As models of small-scale random heterogeneity become more precise, comparisons to geochemical and convection models will become increasingly relevant.

Acknowledgments

Barbara Romanowicz and Sebastian Rost provided helpful comments. This research was supported by National Science Foundation grants EAR-0229323, EAR-0710881, and EAR-1111111.

References

Abubakirov IR and Gusev AA (1990) Estimation of scattering properties of lithosphere of Kamchatka based on Monte-Carlo simulation of record envelope of a near earthquake. *Physics of the Earth and Planetary Interiors* 64: 52–67.

Adams RD (1968) Early reflections of PP as an indication of upper mantle structure. *Bulletin of Seismological Society of America* 58: 1933–1947.

Akamatsu J (1991) Coda attenuation in the Lützow-Holm Bay region, East Antarctica. *Physics of the Earth and Planetary Interiors* 67: 65–75.

Aki K (1969) Analysis of seismic coda of local earthquakes as scattered waves. *Journal of Geophysical Research* 74: 615–631.

Aki K (1973) Scattering of P waves under the Montana LASA. *Journal of Geophysical Research* 78: 1334–1346.

Aki K (1980) Scattering and attenuation of shear waves in the lithosphere. *Journal of Geophysical Research* 85: 6496–6504.

Aki K (1982) Scattering and attenuation. *Bulletin of Seismological Society of America* 72: 319–330.

Aki K and Chouet B (1975) Origin of coda waves: Source attenuation and scattering effects. *Journal of Geophysical Research* 80: 3322–3342.

Aki K and Richards PG (1980) *Quantitative Seismology*. vol. II: San Francisco, CA: W.H. Freeman.

Akinci A, Del Pezzo E, and Ibanez JM (1995) Separation of scattering and intrinsic attenuation in southern Spain and western Anatolia (Turkey). *Geophysical Journal International* 121: 337–353.

Allègre C and Turcotte DL (1986) Implications of a two-component marble-cake mantle. *Nature* 323: 123–127.

Badi G, Del Pezzo E, Ibanez JM, Bianco F, Sabbione N, and Araujo M (2009) Depth dependent seismic scattering in the Nuevo Cuyo region (south central Andes). *Geophysical Research Letters* 36. http://dx.doi.org/10.1029/2009GL041081.

Baig AM and Dahlen FA (2004a) Statistics of traveltimes and amplitudes in random media. *Geophysical Journal International* 158: 187–210.

Baig AM and Dahlen FA (2004b) Traveltime biases in random media and the *S*-wave discrepancy. *Geophysical Journal International* 158: 922–938.

Baig AM, Dahlen FA, and Hung S-H (2003) Traveltimes of waves in three-dimensional random media. *Geophysical Journal International* 153: 467–482.

Bal G and Moscoso M (2000) Polarization effects of seismic waves on the basis of radiative transport theory. *Geophysical Journal International* 142: 571–585.

Bannister SC, Husebye S, and Ruud BO (1990) Teleseismic P coda analyzed by three-component and array techniques: Deterministic location of topographic P-to-Rg scattering near the NORESS array. *Bulletin of Seismological Society of America* 80: 1969–1986.

Baskoutas I (1996) Dependence of coda attenuation on frequency and lapse time in central Greece. *Pure and Applied Geophysics* 147: 483–496.

Baskoutas I and Sato H (1989) Coda attenuation Qc^{-1} for 4 to 64 Hz signals in the shallow crust measured at Ashio, Japan. *Bollettin Della Geofisica Teoreticheskoi Applicata* 21: 277–283.

Bataille K and Flatté SM (1988) Inhomogeneities near the core-mantle boundary inferred from short-period scattered PKP waves recorded at the global digital seismograph network. *Journal of Geophysical Research* 93: 15057–15064.

Bataille K and Lund F (1996) Strong scattering of short-period seismic waves by the core-mantle boundary and the P-diffracted wave. *Geophysical Research Letters* 23: 2413–2416.

Bataille K, Wu RS, and Flatté SM (1990) Inhomogeneities near the core-mantle boundary evidenced from scattered waves: A review. *Pure and Applied Geophysics* 132: 151–173.

Benites R, Aki K, and Yomogida K (1992) Multiple scattering of SH waves in 2D-media with many cavities. *Pure and Applied Geophysics* 138: 353–390.

Benz HM and Vidale JE (1993) The sharpness of upper mantle discontinuities determined from high-frequency *P′P′* precursors. *Nature* 365: 147–150.

Bhattacharyya J, Shearer PM, and Masters TG (1993) Inner core attenuation from short-period PKP(BC) versus PKP(DF) waveforms. *Geophysical Journal International* 114: 1–11.

Bianco F, Del Pezzo E, Castellano M, Ibanez J, and Di Luccio F (2002) Separation of intrinsic and scattering attenuation in the southern Apennines, Italy. *Geophysical Journal International* 150: 10–22.

Bianco F, Del Pezzo E, Malagnini L, Di Luccio F, and Akinci A (2005) Separation of depth-dependent intrinsic and scattering seismic attenuation in the northeastern sector of the Italian peninsula. *Geophysical Journal International* 161: 130–142.

Biswas NN and Aki K (1984) Characteristics of coda waves: Central and southcentral Alaska. *Bulletin of Seismological Society of America* 74: 493–507.

Bolt BA (1962) Gutenberg's early PKP observations. *Nature* 196: 122–124.

Bolt BA (1970) PdP and PKiKP waves and diffracted PcP waves. *Geophysical Journal of the Royal Astronomical Society* 20: 367–382.

Bolt BA, ONeill M, and Qamar A (1968) Seismic waves near 110°: Is structure in core or upper mantle responsible? *Geophysical Journal of the Royal Astronomical Society* 16: 475–487.

Brana L and Helffrich G (2004) A scattering region near the core-mantle boundary under the North Atlantic. *Geophysical Journal International* 158: 625–636.

Bullen KE and Burke-Gaffney TN (1958) Diffracted seismic waves near the PKP caustic. *Geophysical Journal International* 1: 9–17.

Calvet M and Margerin L (2008) Constraints on grain size and stable iron phases in the uppermost inner core from multiple scattering modeling of seismic velocity and attenuation. *Earth and Planetary Science Letters* 267: 200–212. http://dx.doi.org/10.1016/j.epsl.2007.11.048.

Canas JA, Ugalde A, Pujades LG, Carracedo JC, Soler V, and Blanco MJ (1998) Intrinsic and scattering wave attenuation in the Canary Islands. *Journal of Geophysical Research* 103: 15037–15050.

Cao A and Romanowicz B (2007) Locating scatterers in the mantle using array analysis of PKP precursors from an earthquake doublet. *Earth and Planetary Science Letters* 255: 22–31. http://dx.doi.org/10.1016/j.epsl.2006.12.002.

Carcolé E and Sato H (2010) Spatial distribution of scattering loss and intrinsic absorption of short-period *S* waves in the lithosphere of Japan on the basis of the multiple lapse time window analysis of Hi-net data. *Geophysical Journal International* 180: 268–290. http://dx.doi.org/10.1111/j.1365-246X.2009.04394.x.

Castle JC and Creager KC (1999) A steeply dipping discontinuity in the lower mantle beneath Izu-Bonin. *Journal of Geophysical Research* 104: 7279–7292.

Cessaro RK and Butler R (1987) Observations of transverse energy for *P* waves recorded on a deep-ocean borehole seismometer located in the northwest Pacific. *Bulletin of Seismological Society of America* 77: 2163–2180.

Chang AC and Cleary JR (1978) Precursors to *PKKP*. *Bulletin of Seismological Society of America* 68: 1059–1079.

Chang AC and Cleary JR (1981) Scattered *PKKP*: Further evidence for scattering at a rough core-mantle boundary. *Physics of the Earth and Planetary Interiors* 24: 15–29.

Chen X and Long LT (2000) Spatial distribution of relative scattering coefficients determined from microearthquake coda. *Bulletin of Seismological Society of America* 90: 512–524.

Chernov LA (1960) *Wave Propagation in a Random Media*. New York: McGraw-Hill.

Chevrot S, Montagner JP, and Snieder R (1998) The spectrum of tomographic earth models. *Geophysical Journal International* 133: 783–788.

Chung TW, Yoshimoto K, and Yun S (2010) The separation of intrinsic and scattering seismic attenuation in South Korea. *Bulletin of Seismological Society of America* 100: 3183–3193. http://dx.doi.org/10.1785/0120100054.

Cirerone RD, Doll CG, and Toksoz MN (2011) Scattering and attenuation of seismic waves in northeastern North America. *Bulletin of Seismological Society of America* 101: 2897–2903. http://dx.doi.org/10.1785/0120090216.

Cleary J (1981) Seismic wave scattering on underside reflection at the core-mantle boundary. *Physics of the Earth and Planetary Interiors* 26: 266–267.

Cleary JR and Haddon RAW (1972) Seismic wave scattering near the core-mantle boundary: A new interpretation of precursors to PKP. *Nature* 240: 549–551.

Cleary JR, King DW, and Haddon RAW (1975) P-wave scattering in the Earth's crust and upper mantle. *Geophysical Journal of the Royal Astronomical Society* 43: 861–872.

Cormier VF (1995) Time-domain modelling of PKIKP precursors for constraints on the heterogeneity in the lowermost mantle. *Geophysical Journal International* 121: 725–736.

Cormier VF (1999) Anisotropy of heterogeneity scale lengths in the lower mantle from PKIKP precursors. *Geophysical Journal International* 136: 373–384.

Cormier VF (2000) *D″* as a transition in the heterogeneity spectrum of the lowermost mantle. *Journal of Geophysical Research* 105: 16193–16205.

Cormier VF (2007) Texture of the uppermost inner core from forward-and back-scattered seismic waves. *Earth and Planetary Science Letters* 258: 442–453. http://dx.doi.org/10.1016/j.epsl.2007.04.003.

Cormier VF, Attanayake J, and He K (2011) Inner core freezing and melting: Constraints from seismic body waves. *Physics of the Earth and Planetary Interiors* 188: 163–172. http://dx.doi.org/10.1016/j.pepi.2011.07.007.

Cormier VF and Li X (2002) Frequency-dependent seismic attenuation in the inner core 2. A scattering and fabric interpretation. *Journal of Geophysical Research* 107: B12.

Cormier VF, Xu L, and Choy GI (1998) Seismic attenuation in the inner core: Viscoelastic or stratigraphic? *Geophysical Research Letters* 21: 4019–4022.

Dahlen FA, Hung S-H, and Nolet G (2000) Fréchet kernels for finite-frequency traveltimes—I. Theory. *Geophysical Journal International* 141: 157–174.

Dai W and Song X (2008). Detection of Motion and Heterogeneity in Earth's Liquid Outer Core. *Geophysical Research Letters* 35, doi:10.1029/2008GL034895.

Dainty AM (1990) Studies of coda using array and three-component processing. *Pure and Applied Geophysics* 132: 221–244.

Dainty AM, Duckworth RM, and Tie A (1987) Attenuation and backscattering from local coda. *Bulletin of Seismological Society of America* 77: 1728–1747.

Dainty AM and Toksöz MN (1977) Elastic wave propagation in a highly scattering medium—A diffusion approach. *Journal of Geophysics* 43: 375–388.

Dainty AM and Toksöz MN (1981) Seismic codas on the earth and the moon: A comparison. *Physics of the Earth and Planetary Interiors* 26: 250–260.

Dainty AM and Toksöz MN (1990) Array analysis of seismic scattering. *Bulletin of Seismological Society of America* 80: 2242–2260.

Dainty AM, Toksöz MN, Anderson KR, Pines PJ, Nakamura Y, and Latham G (1974) Seismic scattering and shallow structure of the moon in Oceanus Procellarum. *Moon* 91: 11–29.

Dalkolmo J and Friederich W (2000) Born scattering of long-period body waves. *Geophysical Journal International* 142: 867–888.

Davies DJ and Husebye ES (1972) Array analysis of PKP phases and their precursors. *Nature Physical Sciences* 232: 8–13.

Davis JP, Kind R, and Sacks IS (1989) Precursors to *P′P′* re-examined using broad-band data. *Geophysical Journal International* 99: 595–604.

Del Pezzo E, Bianco F, Marzorati S, Augliera P, D'Alema E, and Massa M (2011) Depth-dependent intrinsic and scattering attenuation in north central Italy. *Geophysical Journal International* 186: 373–381. http://dx.doi.org/10.1111/j.1365-246X.2011.05053.x.

Del Pezzo E, De Natale G, Scarcella G, and Zollo A (1985) q_c of three component seismograms of volcanic microearthquakes at Campi Flegrei volcanic area – southern Italy. *Pure and Applied Geophysics* 123: 683–696.

Doornbos DJ (1974) Seismic wave scattering near caustics: Observations of *PKKP* precursors. *Nature* 247: 352–353.

Doornbos DJ (1976) Characteristics of lower mantle inhomogeneities from scattered waves. *Geophysical Journal of the Royal Astronomical Society* 44: 447–470.

Doornbos DJ (1978) On seismic wave scattering by a rough core-mantle boundary. *Geophysical Journal of the Royal Astronomical Society* 53: 643–662.

Doornbos DJ (1980) The effect of a rough core-mantle boundary on *PKKP*. *Physics of the Earth and Planetary Interiors* 21: 351–358.

Doornbos DJ (1988) Multiple scattering by topographic relief with application to the core-mantle boundary. *Geophysical Journal* 92: 465–478.

Doornbos DJ and Husebye ES (1972) Array analysis of PKP phases and their precursors. *Physics of the Earth and Planetary Interiors* 5: 387.

Doornbos DJ and Vlaar NJ (1973) Regions of seismic wave scattering in the Earth's mantle and precursors to PKP. *Nature Physical Science* 243: 58–61.

Earle PS (1999) Polarization of the Earth's teleseismic wavefield. *Geophysical Journal International* 139: 1–8.

Earle PS (2002) Origins of high-frequency scattered waves near PKKP from large aperture seismic array data. *Bulletin of Seismological Society of America* 92: 751–760.

Earle PS, Rost S, Shearer PM, and Thomas C (2011) Scattered *P′P′* waves observed at short distances. *Bulletin of Seismological Society of America* 101: 2843–2854. http://dx.doi.org/10.1785/0120110157.

Earle PS and Shearer PM (1997) Observations of *PKKP* precursors used to estimate small-scale topography on the core-mantle boundary. *Science* 277: 667–670.

Earle PS and Shearer PM (1998) Observations of high-frequency scattered energy associated with the core phase *PKKP*. *Geophysical Research Letters* 25: 405–408.

Earle PS and Shearer PM (2001) Distribution of fine-scale mantle heterogeneity from observations of P_{diff} coda. *Bulletin of Seismological Society of America* 91: 1875–1881.

Emery V, Maupin V, and Nataf H-C (1999) Scattering of *S* waves diffracted at the core-mantle boundary: Forward modelling. *Geophysical Journal International* 139: 325–344.

Engdahl ER and Flinn EA (1969) Seismic waves reflected from discontinuities within Earth's upper mantle. *Science* 163: 177–179.

Fehler M, Hoshiba M, Sato H, and Obara K (1992) Separation of scattering and intrinsic attenuation for the Kanto-Tokai region, Japan, using measurements of *S*-wave energy versus hypocentral distance. *Geophysical Journal International* 198: 787–800.

Fehler M and Sato H (2003) Coda. *Pure and Applied Geophysics* 160: 541–554.

Flatté SM and Wu R-S (1988) Small-scale structure in the lithosphere and asthenosphere deduced from arrival time and amplitude fluctuations at NORSAR. *Journal of Geophysical Research* 93: 6601–6614.

Frankel A (1990) A review of numerical experiments on seismic wave scattering. *Pure and Applied Geophysics* 131: 639–685.

Frankel A and Clayton RW (1984) A finite difference simulation of wave propagation in two-dimensional random media. *Bulletin of Seismological Society of America* 74: 2167–2186.

Frankel A and Clayton RW (1986) Finite difference simulations of seismic scattering: Implications for the propagation of short-period seismic waves in the crust and models of crustal heterogeneity. *Journal of Geophysical Research* 91: 6465–6489.

Frankel A and Wennerberg L (1987) Energy-flux model of seismic coda: Separation of scattering and intrinsic attenuation. *Bulletin of Seismological Society of America* 77: 1223–1251.

Frederiksen AW and Revenaugh J (2004) Lithospheric imaging via teleseismic scattering. *Geophysical Journal International* 159: 978–990.
Frenje L and Juhlin C (2000) Scattering attenuation: 2-D and 3-D finite difference simulations vs. theory. *Journal of Applied Geophysics* 44: 33–46.
Furumura T, Kennett BLN, and Furumura M (1998) Seismic wavefield calculation for laterally heterogeneous whole earth models using the pseudospectral method. *Geophysical Journal International* 135: 845–860.
Gagnepain-Beyneix J (1987) Evidence of spatial variations of attenuation in the western Pyrenean range. *Geophysical Journal of the Royal Astronomical Society* 89: 681–704.
Gao LS, Lee LC, Biswas NN, and Aki K (1983a) Effects of multiple scattering on coda waves in three dimensional medium. *Pure and Applied Geophysics* 121: 3–15.
Gao LS, Lee LC, Biswas NN, and Aki K (1983b) Comparison of the effects between single and multiple scattering on coda waves for local earthquakes. *Bulletin of Seismological Society of America* 73: 377–390.
Garnero EJ (2000) Heterogeneity of the lowermost mantle. *Annual Review of Earth and Planetary Sciences* 28: 509–537.
Giampiccolo E, Gresta A, and Rasconà F (2004) Intrinsic and scattering attenuation from observed seismic codas in south-eastern Sicily (Italy). *Physics of the Earth and Planetary Interiors* 145: 55–66.
Gibson BS and Levander AR (1988) Modeling and processing of scattered waves in seismic reflection surveys. *Geophysics* 53: 466–478.
Goutbeek FH, Dost B, and van Eck T (2004) Intrinsic absorption and scattering attenuation in the southern Netherlands. *Journal of Seismology* 8: 11–23.
Gupta IN and Blandford RR (1983) A mechanism for generation of short-period transverse motion from explosions. *Bulletin of Seismological Society of America* 73: 571–591.
Gupta IN, Lynnes CS, McElfresh TW, and Wagner RA (1990) F-K analysis of NORESS array and single station data to identify sources of near-receiver and near-source scattering. *Bulletin of Seismological Society of America* 80: 2227–2241.
Gupta SC, Teotia SS, Rai SS, and Gautam N (1998) Coda *Q* estimates in the Koyna region, India. *Pure and Applied Geophysics* 153: 713–731.
Gurnis M and Davies F (1986) Mixing in numerical models of mantle convection incorporating plate kinematics. *Journal of Geophysical Research* 91: 6375–6395.
Gusev AA (1995) Vertical profile of turbidity and coda Q. *Geophysical Journal International* 123: 665–672.
Gusev AA and Abubakirov IR (1987) Monte Carlo simulation of record envelope of a near earthquake. *Physics of the Earth and Planetary Interiors* 49: 30–36.
Gusev AA and Abubakirov IR (1999a) Vertical profile of effective turbidity reconstructed from broadening of incoherent body-wave pulses—I. General approach and the inversion procedure. *Geophysical Journal International* 136: 295–308.
Gusev AA and Abubakirov IR (1999b) Vertical profile of effective turbidity reconstructed from broadening of incoherent body-wave pulses—II. Application to Kamchatka data. *Geophysical Journal International* 136: 309–323.
Gutenberg B (1957) The boundary of the Earth's inner core. *Eos, Transactions American Geophysical Union* 38: 750–753.
Gutenberg B and Richter CF (1934) On seismic waves; I. *Gerlands Beitrage zur Geophysik* 43: 56–133.
Gutowski PR and Kanasewich ER (1974) Velocity spectral evidence of upper mantle discontinuities. *Geophysical Journal of the Royal Astronomical Society* 36: 21–32.
Haddon RAW (1972) Corrugations on the CMB or transition layers between the inner and outer cores? (abstract). *Eos, Transactions American Geophysical Union* 53: 600.
Haddon RAW (1982) Evidence for inhomogeneities near the core-mantle boundary. *Philosophical Transactions of the Royal Society London A* 306: 61–70.
Haddon RAW and Cleary JR (1974) Evidence for scattering of seismic PKP waves near the mantle-core boundary. *Physics of the Earth and Planetary Interiors* 8: 211–234.
Haddon RAW, Husebye ES, and King DW (1977) Origin of precursors to PP. *Physics of the Earth and Planetary Interiors* 14: 41–71.
Hedlin MAH and Shearer PM (2000) An analysis of large-scale variations in small-scale mantle heterogeneity using global Seismographic Network recordings of precursors to PKP. *Journal of Geophysical Research* 105: 13655–13673.
Hedlin MAH and Shearer PM (2002) Probing mid-mantle heterogeneity using PKP coda waves. *Physics of the Earth and Planetary Interiors* 130: 195–208.
Hedlin MAH, Shearer PM, and Earle PS (1997) Seismic evidence for small-scale heterogeneity throughout Earth's mantle. *Nature* 387: 145–150.
Helffrich GR and Wood BJ (2001) The Earth's mantle. *Nature* 412: 501–507.
Herraiz M and Espinoa AF (1987) Coda waves: A review. *Pure and Applied Geophysics* 125: 499–577.
Hill RJ (1978) Models of the scalar spectrum for turbulent advection. *Journal of Fluid Mechanics* 88: 541–562.
Hock S, Korn M, Ritter JRR, and Rothert E (2004) Mapping random lithospheric heterogeneities in northern and central Europe. *Geophysical Journal International* 157: 251–264.
Hock S, Korn M, and TOR Working Group (2000) Random heterogeneity of the lithosphere across the Trans-European Suture Zone. *Geophysical Journal International* 141: 57–70.
Holliger K and Levander AR (1992) A stochastic view of lower crustal fabric based on evidence from the Ivrea zone. *Journal of Geophysical Research* 19: 1153–1156.
Hong T-K (2004) Scattering attenuation ratios of *P* and *S* waves in elastic media. *Geophysical Journal International* 158: 211–224.
Hong T-K and Kennett BLN (2003) Scattering attenuation of 2-D elastic waves: Theory and numerical modelling using a wavelet-based method. *Bulletin of Seismological Society of America* 93: 922–938.
Hong T-K, Kennett BLN, and Wu R-S (2004) Effects of the density perturbation in scattering. *Geophysical Research Letters* 31. http://dx.doi.org/10.1029/2004GL019933.
Hong T-K and Menke W (2008) Constituent energy of regional seismic coda. *Bulletin of Seismological Society of America* 98: 454–462. http://dx.doi.org/10.1785/0120070121.
Hong T-K and Wu R-S (2005) Scattering of elastic waves in geometrically anisotropic random media and its implication to sounding of heterogeneity in the Earth's deep interior. *Geophysical Journal International* 163: 324–338.
Hong T-K, Wu R-S, and Kennett BLN (2005) Stochastic features of scattering. *Physics of the Earth and Planetary Interiors* 148: 131–148.
Hoshiba M (1991) Simulation of multiple scattered coda wave excitation based on the energy conservation law. *Physics of the Earth and Planetary Interiors* 67: 123–136.
Hoshiba M (1993) Separation of scattering attenuation and intrinsic absorption in Japan using the multiple lapse time window analysis of full seismogram envelope. *Journal of Geophysical Research* 98: 15809–15824.
Hoshiba M (1994) Simulation of coda wave envelope in depth dependent scattering and absorption structure. *Geophysical Research Letters* 21: 2853–2856.
Hoshiba M (1997) Seismic coda wave envelope in depth-dependent *S* wave velocity structure. *Physics of the Earth and Planetary Interiors* 104: 15–22.
Hoshiba M, Rietbrock A, Scherbaum F, Nakahara H, and Haberland C (2001) Scattering attenuation and intrinsic absorption using uniform and depth dependent model—Application to full seismogram envelope recorded in northern Chile. *Journal of Seismology* 5: 157–179.
Hudson JA and Heritage JR (1981) Use of the Born approximation in seismic scattering problems. *Geophysical Journal of the Royal Astronomical Society* 66: 221–240.
Husebye ES, Haddon RAW, and King DW (1977) Precursors to PP and upper mantle discontinuities. *Journal of Geophysical Research* 43: 535–543.
Husebye ES, King DW, and Haddon RAW (1976) Precursors to PKIKP and seismic wave scattering near the mantle-core boundary. *Journal of Geophysical Research* 81: 1870–1882.
Husebye E and Madariaga R (1970) The origin of precursors to core waves. *Bulletin of Seismological Society of America* 60: 939–952.
Jahnke G, Thorne MS, Cochard A, and Igel H (2008) Global SH-wave propagation using a parallel axisymmetric spherical finite-difference scheme: Application to whole mantle scattering. *Geophysical Journal International* 173: 815–826. http://dx.doi.org/10.1111/j/1365-246X.2008.03744.x.
Jemberie AL and Nyblade AA (2009) Intrinsic and scattering Q near 1 Ha across the East African Plateau. *Bulletin of Seismological Society of America* 99: 3516–3524. http://dx.doi.org/10.1785/0120090062.
Jin A and Aki K (1988) Spatial and temporal correlation between coda Q and seismicity in China. *Bulletin of Seismological Society of America* 78: 741–769.
Jin A, Cao T, and Aki K (1985) Regional change of coda Q in the oceanic lithosphere. *Journal of Geophysical Research* 90: 8651–8659.
Jin A, Mayeda K, Adams D, and Aki K (1994) Separation of intrinsic and scattering attenuation in southern California using TERRAscope data. *Journal of Geophysical Research* 99: 17835–17848.
Kaelin B and Johnson LR (1998) Dynamic composite elastic medium theory, 2, three-dimensional media. *Journal of Applied Physics* 84: 5458–5468.
Kampfmann W and Muüller G (1989) PcP amplitude calculations for a core-mantle boundary with topography. *Geophysical Research Letters* 16: 653–656.
Kaneshima S (2003) Small-scale heterogeneity at the top of the lower mantle around the Mariana slab. *Earth and Planetary Science Letters* 209: 85–101.
Kaneshima S (2009) Seismic scatterers at the shallowest lower mantle beneath sub ducted slabs. *Earth and Planetary Science Letters* 286: 304–315. http://dx.doi.org/10.1016/j.epsl.2009.06.044.
Kaneshima S and Helffrich G (1998) Detection of lower mantle scatterers northeast of the Mariana subduction zone using short-period array data. *Journal of Geophysical Research* 103: 4825–4838.
Kaneshima S and Helffrich G (1999) Dipping low-velocity layer in the mid-lower mantle: Evidence for geochemical heterogeneity. *Science* 283: 1888–1892.

Kaneshima S and Helffrich G (2003) Subparallel dipping heterogeneities in the mid-lower mantle. *Journal of Geophysical Research* 108. http://dx.doi.org/10.1029/2001JB001596.

Kaneshima S and Helffrich G (2009) Lower mantle scattering profiles and fabric below Pacific subduction zones. *Earth and Planetary Science Letters* 282: 234–239. http://dx.doi.org/10.1016/j.epsl.2009.03.024.

Kaneshima S and Helffrich G (2010) Small scale heterogeneity in the mid-lower mantle beneath the circum-Pacific area. *Physics of the Earth and Planetary Interiors* 183: 91–103. http://dx.doi.org/10.1016/j.pepi.2010.03.011.

King DW and Cleary JR (1974) A note on the interpretation of precursors to PKPPKP. *Bulletin of Seismological Society of America* 64: 721–723.

King DW, Haddon RAW, and Cleary JR (1973) Evidence for seismic wave scattering in the *D″* layer. *Earth and Planetary Science Letters* 20: 353–356.

King DW, Haddon RAW, and Cleary JR (1974) Array analysis of precursors to PKIKP in the distance range 128° to 142°. *Geophysical Journal of the Royal Astronomical Society* 37: 157–173.

King DW, Haddon RAW, and Husebye ES (1975) Precursors to PP. *Physics of the Earth and Planetary Interiors* 10: 103–127.

Knopoff L and Hudson JA (1964) Scattering of elastic waves by small inhomogeneities. *Journal of the Acoustical Society of America* 36: 338–343.

Koper KD and Dombrovskaya M (2005) Seismic properties of the inner core boundary from PKiKP/P amplitude ratios. *Earth and Planetary Science Letters* 237: 680–694.

Koper KD, Franks JM, and Dombrovskaya M (2004) Evidence for small-scale heterogeneity in Earth's inner core from a global study of PKiKP coda waves. *Earth and Planetary Science Letters* 228: 227–241.

Kopnichev YF (1977) The role of multiple scattering in the formulation of a seismogram's tail. *Izy. Acad. Nauk USSR (Engl. Trans. Physics of the Solid Earth)* 13: 394–398.

Korn M (1988) P-wave coda analysis of short-period array data and the scattering and absorptive properties of the lithosphere. *Geophysical Journal* 93: 437–449.

Korn M (1990) A modified energy flux model for lithospheric scattering of teleseismic body waves. *Geophysical Journal International* 102: 165–175.

Korn M (1993) Determination of site-dependent scattering Q from P-wave coda analysis with an energy flux model. *Geophysical Journal International* 113: 54–72.

Korn M (1997) Modelling the teleseismic P coda envelope: Depth dependent scattering and deterministic structure. *Physics of the Earth and Planetary Interiors* 104: 23–36.

Korn M and Sato H (2005) Synthesis of plane vector wave envelopes in two-dimensional random elastic media based on the Markov approximation and comparison with finite-difference synthetics. *Geophysical Journal International* 161: 839–848.

Korneev VA and Johnson LR (1993a) Scattering of elastic waves by a spherical inclusion—I. Theory and numerical results. *Geophysical Journal International* 115: 230–250.

Korneev VA and Johnson LR (1993b) Scattering of elastic waves by a spherical inclusion—II. Limitations of asymptotic solutions. *Geophysical Journal International* 115: 251–263.

Kosuga M (1992) Determination of coda *Q* on frequency and lapse time in the western Nagano region, Japan. *Journal of Physics of the Earth* 40: 421–445.

Kosuga M (1997) Periodic ripple of coda envelope observed in northeastern Japan. *Physics of the Earth and Planetary Interiors* 104: 91–108.

Krasnoshchekov DN, Kaazik PB, and Ovtchinnikov VM (2005) Seismological evidence for mosaic structure of the surface of the Earth's inner core. *Nature* 435: 483–487. http://dx.doi.org/10.1038/nature03613.

Krüger FK, Baumann M, Scherbaum F, and Weber M (2001) Mid mantle scatterers near the Mariana slab detected with a double array method. *Geophysical Research Letters* 28: 667–670.

Kvamme LB and Havskov J (1989) Q in southern Norway. *Bulletin of Seismological Society of America* 79: 1575–1588.

Lacombe C, Campillo M, Paul A, and Margerin L (2003) Separation of intrinsic absorption and scattering attenuation from Lg coda decay in central France using acoustic radiative transfer theory. *Geophysical Journal International* 154: 417–425.

Langston GA (1989) Scattering of teleseismic body waves under Pasadena, California. *Journal of Geophysical Research* 94: 1935–1951.

Lay T (1987) Analysis of near-source contributions to early *P*-wave coda for underground explosions. II. Frequency dependence. *Bulletin of Seismological Society of America* 77: 1252–1273.

Lee WS, Sato H, and Lee K (2003) Estimation of *S*-wave scattering coefficient in the mantle from envelope characteristics before and after the ScS arrival. *Geophysical Research Letters* 30: 24. http://dx.doi.org/10.1029/2003GL018413.

Lee WS, Sato H, and Lee K (2006) Scattering coefficients in the mantle revealed from the seismogram envelope analysis based on the multiple isotropic scattering model. *Earth and Planetary Science Letters* 2006: 888–900. http://dx.doi.org/10.1016/j/epsl.2005.10.035.

Lee WS, Yun S, and Do J-Y (2010) Scattering and intrinsic attenuation of short-period *S* waves in the Gyeongsang Basin, South Korea, revealed from S-wave seismogram envelopes based on the radiative transfer theory. *Bulletin of Seismological Society of America* 100: 833–840. http://dx.doi.org/10.1785/0120090149.

Lerche I and Menke W (1986) An inversion method for separating apparent and intrinsic attenuation in layered media. *Geophysical Journal of the Royal Astronomical Society* 87: 333–347.

Levander AR and Hill NR (1985) P-SV resonances in irregular low-velocity surface layers. *Bulletin of Seismological Society of America* 75: 847–864.

Levander A, Hobbs RW, Smith SK, England RW, Snyder DB, and Holliger K (1994) The crust as a heterogeneous "optical" medium, or "crocodiles in the mist". *Tectonophysics* 232: 281–297.

Leyton F and Koper KD (2007a) Using PKiKp coda to determine inner core structure: 1. Synthesis of coda envelopes using single scattering theories. *Journal of Geophysical Research* 112. http://dx.doi.org/10.1029/2006JB004369.

Leyton F and Koper KD (2007b) Using PKiKp coda to determine inner core structure: 2. Determination of Qc. *Journal of Geophysical Research* 112. http://dx.doi.org/10.1029/2006JB004370.

Malin PE and Phinney RA (1985) On the relative scattering of P and S waves. *Geophysical Journal of the Royal Astronomical Society* 80: 603–618.

Mancinelli NJ and Shearer PM (2013) Reconciling discrepancies among estimates of small-scale mantle heterogeneity from PKP precursors. *Geophysical Journal International* 195: 1721–1729. http://dx.doi.org/10.1093/gji/ggt319.

Margerin L (2004) Introduction to radiative transfer of seismic waves. *Seismic Data Analysis and Imaging with Global and Local Arrays. AGU Monograph Series.* Washington DC: American Geophysical Union.

Margerin L (2006) Attenuation, transport and diffusion of scalar waves in textured random media. *Tectonophysics* 416: 229–244. http://dx.doi.org/10.1016/j.tecto.2005.11.011.

Margerin L (2013) Diffusion approximation with polarization and resonance effects for the modeling of seismic waves in strongly scattering small-scale media. *Geophysical Journal International* http://dx.doi.org/10.1093/gji/ggs022.

Margerin L, Campillo M, Shapiro NM, and van Tiggelen BA (1999) Residence time of diffuse waves in the crust as a physical interpretation of coda Q: Application to seismograms recorded in Mexico. *Geophysical Journal International* 138: 343–352.

Margerin L, Campillo M, and van Tiggelen BA (1998) Radiative transfer and diffusion of waves in a layered medium: New insight into coda Q. *Geophysical Journal International* 134: 596–612.

Margerin L, Campillo M, and van Tiggelen B (2000) Monte Carlo simulation of multiple scattering of elastic waves. *Journal of Geophysical Research* 105: 7873–7892.

Margerin L, Campillo M, and van Tiggelen B (2001) Effect of absorption on energy partition of elastic waves. *Bulletin of Seismological Society of America* 91: 624–627.

Margerin L, Campillo M, van Tiggelen B, and Hennino R (2009) Energy partition of seismic coda waves in layered media: Theory and application to Pinyon Flats Observatory. *Geophysical Journal International* 177: 571–585. http://dx.doi.org/10.1111/j.1365-246X.2008.04068.x.

Margerin L and Nolet G (2003a) Multiple scattering of high-frequency seismic waves in the deep Earth: Modeling and numerical examples. *Journal of Geophysical Research* 108: B5. http://dx.doi.org/10.1029/2002JB001974.

Margerin L and Nolet G (2003b) Multiple scattering of high-frequency seismic waves in the deep Earth: PKP precursor analysis and inversion for mantle granularity. *Journal of Geophysical Research* 108: B11. http://dx.doi.org/10.1029/2003JB002455.

Margerin L, van Tiggelen B, and Campillo M (2001) Effect of absorption on energy partition of elastic waves in the seismic coda. *Bulletin of Seismological Society of America* 91: 624–627.

Matsumoto S (1995) Characteristics of coda waves and inhomogeneity of the earth. *Journal of Physics of the Earth* 43: 279–299.

Matsumoto S (2005) Scatterer density estimation in the crust by seismic array processing. *Geophysical Journal International* http://dx.doi.org/10.1111/j.1365-246X.2005.02773.x.

Matsumoto S and Hasegawa A (1989) Two-dimensional coda *Q* structure beneath Tohoku, NE Japan. *Geophysical Journal International* 99: 101–108.

Mayeda K, Koyanagi S, Hoshiba M, Aki K, and Zeng Y (1992) A comparative study of scattering, intrinsic, and coda Q^{-1} for Hawaii, Long Valley, and central California between 1.5 and 15.0 Hz. *Journal of Geophysical Research* 97: 6643–6659.

Mayeda K, Su F, and Aki K (1991) Seismic albedo from the total seismic energy dependence on hypocentral distances in southern California. *Physics of the Earth and Planetary Interiors* 67: 104–114.

McLaughlin KL and Anderson LM (1987) Stochastic dispersion of short-period *P*-waves due to scattering and multipathing. *Geophysical Journal of the Royal Astronomical Society* 89: 933–964.

McLaughlin KL, Anderson LM, and Der Z (1985) Investigation of seismic waves using 2-dimensional finite difference calculations. In: *Multiple Scattering of Seismic Waves in Random Media and Random Surfaces*, pp. 795–821. Pennsylvania State University.

Meibom A and Anderson DL (2003) The statistical upper mantle assemblage. *Earth and Planetary Science Letters* 217: 123–139.

Miller MS and Niu F (2008) Bulldozing the core-mantle boundary: Localized seismic scatterers beneath the Caribbean Sea. *Physics of the Earth and Planetary Interiors* 170: 89–94. http://dx.doi.org/10.1016/j.pepi.2008.07.044.

Morgan JP and Morgan WJ (1999) Two-stage melting and the geochemical evolution of the mantle: A recipe for mantle plum-pudding. *Earth and Planetary Science Letters* 170: 215–239.

Morozov IB, Morozova EA, Smithson SB, and Solodilov LN (1998) On the nature of the teleseismic Pn phase observed on the ultralong-range profile Quartz, Russia. *Bulletin of Seismological Society of America* 88: 62–73.

Morozov IB and Smithson SB (2000) Coda of long-range arrivals from nuclear explosions. *Bulletin of Seismological Society of America* 90: 929–939.

Mukhopadhyay S and Tyagi C (2008) Variation of intrinsic and scattering attenuation with depth in NW Himalayas. *Geophysical Journal International* 172: 1055–1065. http://dx.doi.org/10.1111/j/1365-246X.2007.03688.x.

Müller TM and Shapiro SA (2003) Amplitude fluctuations due to diffraction and reflection in anisotropic random media: Implications for seismic scattering attenuation estimates. *Geophysical Journal International* 155: 139–148.

Nakamura Y (1977) Seismic energy transmission in an intensively scattering environment. *Journal of Geophysical Research* 43: 389–399.

Nakanishi I (1990) High-frequency waves following PKP-Cdiff at distances greater than 155°. *Geophysical Research Letters* 17: 639–642.

Neele F and Snieder R (1991) Are long-period body wave coda caused by lateral heterogeneity? *Geophysical Journal International* 107: 131–153.

Nguyen-Hai (1963) Propagation des ondes longitudinales dans le noyau terrestre. *Annals of Geophysics* 15: 285–346.

Nielsen L and Thybo H (2003) The origin of teleseismic *Pn* waves: Multiple crustal scattering of upper mantle whispering gallery phases. *Journal of Geophysical Research* 108. http://dx.doi.org/10.1029/2003JB002487.

Nielsen L and Thybo H (2006) Identification of crustal and upper mantle heterogeneity by modeling of controlled source seismic data. *Tectonophysics* 416: 209–228. http://dx.doi.org/10.1016/j/tecto/2005.11.020.

Nielsen L, Thybo H, Levander A, and Solodilov LN (2003) Origin of upper-mantle seismic scattering – Evidence from Russian peaceful nuclear explosion data. *Geophysical Journal International* 154: 196–204.

Nielsen L, Thybo H, Morozov B, Smithson SB, and Solodilov L (2003) Teleseismic Pn arrivals: Influence of upper mantle velocity gradient and crustal scattering. *Geophysical Journal International* 153: F1–F7.

Nishigami K (1991) A new inversion method of coda waveforms to determine spatial distribution of coda scatterers in the crust and uppermost mantle. *Geophysical Research Letters* 18: 2225–2228.

Nishigami K (1997) Spatial distribution of coda scatterers in the crust around two active volcanoes and one active fault system in central Japan: Inversion analysis of coda envelope. *Physics of the Earth and Planetary Interiors* 104: 75–89.

Nishimura T, Yoshimoto K, Ohtaki T, Kanjo K, and Purwana I (2002) Spatial distribution of lateral heterogeneity in the upper mantle around the western Pacific region as inferred from analysis of transverse components of teleseismic P-coda. *Geophysical Research Letters* 29: 2137. http://dx.doi.org/10.1029/2002GL015606.

Niu F and Kawakatsu H (1994) Seismic evidence for a 920-km discontinuity in the mantle. *Nature* 371: 301–305.

Niu F and Kawakatsu H (1997) Depth variation of the mid-mantle discontinuity. *Geophysical Research Letters* 24: 429–432.

Niu F and Wen L (2001) Strong seismic scatterers near the core-mantle boundary west of Mexico. *Geophysical Research Letters* 28: 3557–3560.

Nolet G, Dahlen FA, Montelli R, Nolet G, Dahlen FA, and Montelli R (2005) Travel times and amplitudes of seismic waves: A re-assessment. In: *Seismic Earth: Analysis of Broadband Seismograms*, *AGU Monograph Series*, pp. 37–48.

Oancea V, Bazacliu O, and Mihalache G (1991) Estimation of the coda quality factor for the Romanian territory. *Physics of the Earth and Planetary Interiors* 67: 87–94.

Obara K (1997) Simulations of anomalous seismogram envelopes at coda portions. *Physics of the Earth and Planetary Interiors* 104: 109–125.

Obara K and Sato H (1995) Regional differences of random heterogeneities around the volcanic front in the Kanto-Tokai area, Japan revealed from the broadening of *S* wave seismogram envelopes. *Journal of Geophysical Research* 100: 2103–2121.

Olson P, Yuen DA, and Balsiger D (1984) Convective mixing and the fine structure of mantle heterogeneity. *Physics of the Earth and Planetary Interiors* 36: 291–304.

Padhy S and Subhadra N (2010) Attenuation of high-frequency seismic waves in northeastern India. *Geophysical Journal International* 181: 453–467. http://dx.doi.org/10.1111/j/1365-246X.2010.04502.x.

Padhy S, Subhadra N, and Kayal JR (2011) Frequency-dependent attenuation of body and coda waves in the Andaman Sea Basin. *Bulletin of Seismological Society of America* 101: 109–125. http://dx.doi.org/10.1785/0120100032.

Papanicolaou G, Ryshik L, and Keller J (1996) On the stability of the P to S energy ratio in the diffusive regime. *Bulletin of Seismological Society of America* 86: 1107–1115, see also erratum in, Bulletin of Seismological Society of America, 86, p. 1997.

Peng Z, Koper KD, Vidale JE, Leyton F, and Shearer P (2008) Inner-core fine-scale structure from scattered waves recorded by LASA. *Journal of Geophysical Research* 113. http://dx.doi.org/10.1029/2007JB005412.

Poupinet G and Kennett BLN (2004) On the observation of high frequency PKiKP and its coda in Australia. *Physics of the Earth and Planetary Interiors* 146: 497–511.

Przybilla J and Korn M (2008) Monte Carlo simulation of radiative energy transfer in continuous elastic random media – Three-component envelopes and numerical validation. *Geophysical Journal International* 173: 566–576. http://dx.doi.org/10.1111/j/1365-246.2008.03747.x.

Przybilla J, Korn M, and Wegler U (2006) Radiative transfer of elastic waves versus finite difference simulations in two-dimensional random media. *Journal of Geophysical Research* 111. http://dx.doi.org/10.1029/2005JB003952.

Pulli JJ (1984) Attenuation of coda waves in New England. *Bulletin of Seismological Society of America* 74: 1149–1166.

Rautian TG and Khalturin VI (1978) The use of coda for determination of the earthquake source spectrum. *Bulletin of Seismological Society of America* 68: 923–948.

Revenaugh J (1995) The contribution of topographic scattering to teleseismic coda in southern California. *Geophysical Research Letters* 22: 543–546.

Revenaugh J (1999) Geologic applications of seismic scattering. *Annual Review of Earth and Planetary Sciences* 27: 55–73.

Revenaugh J (2000) The relation of crustal scattering to seismicity in southern California. *Journal of Geophysical Research* 105: 25403–25422.

Rhea S (1984) Q determined from local earthquakes in the south Carolina coastal plain. *Bulletin of Seismological Society of America* 74: 2257–2268.

Richards PG (1972) Seismic waves reflected from velocity gradient anomalies within the Earth's mantle. *Zeitschrift für Geophysik* 38: 517–527.

Richards PG and Menke W (1983) The apparent attenuation of a scattering medium. *Bulletin of Seismological Society of America* 73: 1005–1022.

Ritter JRR, Mai PM, Stoll G, and Fuchs K (1997) Scattering of teleseismic waves in the lower crust observations in the Massif Central, France. *Physics of the Earth and Planetary Interiors* 104: 127–146.

Ritter JRR and Rothert E (2000) Variations of the lithospheric seismic scattering strength below the Massif Central, France and the Frankonian Jura, SE Germany. *Tectonophysics* 328: 297–305.

Ritter JRR, Shapiro SA, and Schechinger B (1998) Scattering parameters of the lithosphere below the Massif Central, France, from teleseismic wavefield records. *Geophysical Journal International* 134: 187–198.

Rodriguez M, Havskov J, and Singh SK (1983) Q from coda waves near Petatlán, Guerrero, Mexico. *Bulletin of Seismological Society of America* 73: 321–326.

Roecker SW, Tucker B, King J, and Hatzfeld D (1982) Estimates of Q in central Asia as a function of frequency and depth using the coda of locally recorded earthquakes. *Bulletin of Seismological Society of America* 72: 129–149.

Rost S and Earle PS (2010) Identifying regions of strong scattering at the core-mantle boundary from analysis of *PKKP* precursor energy. *Earth and Planetary Science Letters* 297: 616–626. http://dx.doi.org/10.1016/j.epsl.2010.07.014.

Rost S, Garnero EJ, and Williams Q (2008) Seismic array detection of subducted oceanic crust in the lower mantle. *Journal of Geophysical Research* 113. http://dx.doi.org/10.1029/2007JB005263.

Rost S, Thorne MS, and Garnero EJ (2006) Imaging global seismic phase arrivals by stacking array processed short-period data. *Seismological Research Letters* 77: 697–707.

Roth M and Korn M (1993) Single scattering theory versus numerical modelling in 2-D random media. *Geophysical Journal International* 112: 124–140.

Rothert E and Ritter JRR (2000) Small-scale heterogeneities below the Gräfenberg array, Germany from seismic wavefield fluctuations of Hindu Kish events. *Geophysical Journal International* 140: 175–184. http://dx.doi.org/10.1046/j.1365-246x.2000.00013.x.

Ryberg T, Fuchs K, Egorkin V, and Solodilov L (1995) Observation of high-frequency teleseismic Pn waves on the long-range Quartz profile across northern Eurasia. *Journal of Geophysical Research* 100: 18151–18163.

Ryberg T, Tittgemeyer M, and Wenzel F (2000) Finite difference modelling of *P*-wave scattering in the upper mantle. *Geophysical Journal International* 141: 787–800.

Ryzhik LV, Papanicolaou GC, and Keller JB (1996) Transport equations for elastics and other waves in random media. *Wave Motion* 24: 327–370.

Sacks IS and Saa G (1969) The structure of the transition zone between the inner core and the outer core. *Year Book*, vol. 69, pp. 419–426. Washington: Carnegie Inst.

Saito T, Sato H, Fehler M, and Ohtake M (2003) Simulating the envelope of scalar waves in 2D random media having power-law spectra of velocity fluctuation. *Bulletin of Seismological Society of America* 93: 240–252.

Saito T, Sato H, and Ohtake M (2002) Envelope broadening of spherically outgoing waves in three-dimensional random media having power law spectra. *Journal of Geophysical Research* 107. http://dx.doi.org/10.1029/2001JB000264.

Sato H (1977) Energy propagation including scattering effects, single isotropic scattering approximation. *Journal of Physics of the Earth* 25: 27–41.

Sato H (1978) Mean free path of *S*-waves under the Kanto district of Japan. *Journal of Physics of the Earth* 26: 185–198.

Sato H (1984) Attenuation and envelope formation of three-component seismograms of small local earthquakes in randomly inhomogeneous lithosphere. *Journal of Geophysical Research* 89: 1221–1241.

Sato H (1989) Broadening of seismogram envelopes in the randomly inhomogeneous lithosphere based on the parabolic approximation: Southeast Honshu, Japan. *Journal of Geophysical Research* 94: 17735–17747.

Sato H (1990) Unified approach to amplitude attenuation and coda excitation in the randomly inhomogeneous litho-sphere. *Pure and Applied Geophysics* 132: 93–121.

Sato H (1991) Study of seismogram envelopes based on scattering by random inhomogeneities in the lithosphere: A review. *Physics of the Earth and Planetary Interiors* 67: 4–19.

Sato H (1993) Energy transportation in one- and two-dimensional scattering media: Analytic solutions of the multiple isotropic scattering model. *Geophysical Journal International* 112: 141–146.

Sato H (1994) Multiple isotropic scattering model including P-S conversions for the seismogram envelope formulation. *Geophysical Journal International* 117: 487–494.

Sato H and Fehler MC (1998) *Seismic Wave Propagation and Scattering in the Heterogeneous Earth*. New York: Springer-Verlag.

Sato H, Fehler M, and Saito T (2004) Hybrid synthesis of scalar wave envelopes in two-dimensional random media having rich short-wavelength spectra. *Journal of Geophysical Research* 109. http://dx.doi.org/10.1029/2003JB002673.

Sato H, Nakahara H, and Ohtake M (1997) Synthesis of scattered energy density for nonspherical radiation from a point shear-dislocation source based on the radiative transfer theory. *Physics of the Earth and Planetary Interiors* 104: 1–13.

Sato H and Nishino M (2002) Multiple isotropic-scattering model on the spherical Earth for the synthesis of Rayleigh-wave envelopes. *Journal of Geophysical Research* 107: 2343. http://dx.doi.org/10.1029/2001JB000915.

Scherbaum F, Gilard D, and Deichmann N (1991) Slowness power analysis of the coda composition of two microearthquake clusters in northern Switzerland. *Physics of the Earth and Planetary Interiors* 67: 137–161.

Scherbaum F, Krüger F, and Wever M (1997) Double beam imaging: Mapping lower mantle heterogeneities using combinations of source and receiver arrays. *Journal of Geophysical Research* 102: 507–522.

Scherbaum F and Sato H (1991) Inversion of full seismogram envelopes based on the parabolic approximation: Estimation of randomness and attenuation in southeast Honshu, Japan. *Journal of Geophysical Research* 96: 2223–2232.

Schisselé E, Guilbert J, Gaffet S, and Cansi Y (2004) Accurate time-frequency-wavenumber analysis to study coda waves. *Geophysical Journal International* 158: 577–591.

Shang T and Gao L (1988) Transportation theory of multiple scattering and its application to seismic coda waves of impulsive source. *Scientia Sinica* 31: 1503–1514.

Shapiro NM, Campillo M, Margerin L, Singh SK, Kostoglodov V, and Pacheco J (2000) The energy partitioning and the diffusive character of the seismic coda. *Bulletin of Seismological Society of America* 90: 655–665.

Shapiro SA and Kneig G (1993) Seismic attenuation by scattering: Theory and numerical results. *Geophysical Journal International* 114: 373–391.

Shapiro SA, Schwarz R, and Gold N (1996) The effect of random isotropic inhomogeneities on the phase velocity of seismic waves. *Geophysical Journal International* 114: 373–391.

Shearer PM (1990) Seismic imaging of upper-mantle structure with new evidence for a 520-km discontinuity. *Nature* 344: 121–126.

Shearer PM (1991) Constraints on upper-mantle discontinuities from observations of long-period reflected and converted phases. *Journal of Geophysical Research* 96: 18147–18182.

Shearer PM and Earle PS (2004) The global short-period wavefield modelled with a Monte Carlo seismic phonon method. *Geophysical Journal International* 158: 1103–1117.

Shearer PM and Earle PS (2008) Observing and modeling elastic scattering in the deep Earth. *Advances in Geophysics* 150: 167–193. http://dx.doi.org/10.1016/S0065-2687(08)00006-X (Chapter 6).

Shearer PM, Hedlin MAH, and Earle PS (1998) PKP and PKKP precursor observations: Implications for the small-scale structure of the deep mantle and core. In: *The Core-Mantle Boundary Region*. *Geodynamics*, 28, pp. 37–55. American Geophysical Union.

Shearer PM and Masters TG (1990) The density and shear velocity contrast at the inner core boundary. *Geophysical Journal International* 102: 491–498.

Singh DD, Govoni A, and Bragato PL (2001) Coda Qc attenuation and source parameter analysis in Friuli (NE Italy) and its vicinity. *Pure and Applied Geophysics* 158: 1737–1761.

Singh S and Herrmann RB (1983) Regionalization of crustal coda Q in the continental Unites States. *Journal of Geophysical Research* 88: 527–538.

Song XD and Richards PG (1996) Seismological evidence for differential rotation of the Earth's inner core. *Nature* 382: 221–224.

Spetzler J and Snieder R (2001) The effect of small-scale heterogeneity on the arrival time of waves. *Geophysical Journal International* 145: 786–796.

Spudich P and Bostwick T (1987) Studies of the seismic coda using an earthquake cluster as a deeply buried seismography array. *Journal of Geophysical Research* 92: 10526–10546.

Spudich P and Iida M (1993) The seismic coda, site effects, and scattering in alluvial basins studied using aftershocks of the 1986 North Palm Springs, California, earthquake as source arrays. *Bulletin of Seismological Society of America* 83: 1721–1743.

Spudich P and Miller DP (1990) Seismic site effects and the spatial interpolation of earthquake seismograms: Results using aftershocks of the 1986 North Palm Springs, California, earthquake. *Bulletin of Seismological Society of America* 80: 1504–1532.

Su W-J and Dziewonski AM (1991) Predominance of long-wavelength heterogeneity in the mantle. *Nature* 352: 121–126.

Taira T and Yomogida K (2004) Imaging of three-dimensional small-scale heterogeneities in the Hidaka, Japan region: A coda spectral analysis. *Geophysical Journal International* 158: 998–1008.

Takahashi T (2012) Three-dimensional attenuation structure of intrinsic absorption and wide-angle scattering of *S* waves in northeastern Japan. *Geophysical Journal International* 189: 1667–1680. http://dx.doi.org/10.1111/j.1365-246X.2012.05438.x.

Tanaka S (2005) Characteristics of PKP-Cdiff coda revealed by small-aperture seismic arrays: Implications for the study of the inner core boundary. *Physics of the Earth and Planetary Interiors* 153: 49–60.

Thomas C, Igel H, Weber M, and Scherbaum F (2000) Acoustics simulation of *P*-wave propagation in a heterogeneous spherical earth; numerical method and application to precursor wave to PKP*df*. *Geophysical Journal International* 141: 307–320.

Thomas C, Kendall J-M, and Helffrich G (2009) Probing two low-velocity regions with PKP b-caustic amplitudes and scattering. *Geophysical Journal International* 178: 503–512. http://dx.doi.org/10.1111/j.1365-246X.2009.04189.x.

Thomas C, Weber M, Wicks CW, and Scherbaum F (1999) Small scatterers in the lower mantle observed at German broadband arrays. *Journal of Geophysical Research* 104: 15073–15088.

Tittgemeyer MF, Wenzel F, Fuchs K, and Ryberg T (1996) Wave propagation in a multiple-scattering upper mantle: Observations and modeling. *Geophysical Journal International* 127: 492–502.

Tkalčić H, Cormier VF, Kennett BLN, and He K (2010) Steep reflections from the earth's core reveal small-scale heterogeneity in the upper mantle. *Physics of the Earth and Planetary Interiors* 178: 80–91. http://dx.doi.org/10.1016/j.pepi.2009.08.004.

Tkalčić H, Flanagan M, and Cormier VF (2006) Observation of near-podal *P′P′* precursors: Evidence for back scattering from the 150–220 km zone in the Earth's upper mantle. *Geophysical Research Letters* 33. http://dx.doi.org/10.1029/2005GL024626.

Toksöz NM, Daity AM, Reiter E, and Wu RS (1988) A model for attenuation and scattering in the earth's crust. *Pure and Applied Geophysics* 128: 81–100.

Tono Y and Yomogida K (1996) Complex scattering at the core-mantle boundary observed in short-period diffracted P-waves. *Journal of Physics of the Earth* 44: 729–744.

Tono Y and Yomogida K (1997) Origin of short-period signals following P-diffracted waves: A case study of the 1994 Bolivian deep earthquake. *Physics of the Earth and Planetary Interiors* 103: 1–16.
Torquato S (2002) *Random Heterogeneous Materials: Microscopic and Macroscopic Properties*. New York: Springer.
Tsuruga K, Yomogida K, Ito H, and Nishigami K (2003) Detection of localized small-scale heterogeneities in the Hanshin-Awaji region, Japan, by anomalous amplification of coda level. *Bulletin of Seismological Society of America* 93: 1516–1530.
Ugalde A, Pujades LG, Canas JA, and Villasenor A (1998) Estimation of the intrinsic absorption and scattering attenuation in northeastern Venezuela (southern Caribbean) using coda waves. *Pure and Applied Geophysics* 153: 685–702.
Ugalde A, Vargas CA, Pujades LG, and Canas JA (2002) Seismic coda attenuation after the Mw = 6.2 Armenia (Columbia) earthquake of 25 January 1999. *Journal of Geophysical Research:* 107. http://dx.doi.org/10.1029/2001JB000197.
van Eck T (1988) Attenuation of coda waves in the dead sea region. *Bulletin of Seismological Society of America* 78: 770–779.
Vargas CA, Ugalde A, Pujades LG, and Canas JA (2004) Spatial variation of coda wave attenuation in northwestern Columbia. *Geophysical Journal International* 158: 609–624.
Vidale JE and Benz HM (1992) A sharp and flat section of the core-mantle boundary. *Nature* 359: 627–629.
Vidale JE, Dodge DA, and Earle PS (2000) Slow differential rotation of the Earth's inner core indicated by temporal changes in scattering. *Nature* 405: 445–448.
Vidale JE and Earle PS (2000) Fine-scale heterogeneity in the Earth's inner core. *Nature* 404: 273–275.
Vidale JE and Earle PS (2005) Evidence for inner-core rotation from possible changes with time in PKP coda. *Geophysical Research Letters* 32. http://dx.doi.org/10.1029/2004GL021240.
Vidale JE and Hedlin MAH (1998) Evidence for partial melt at the core-mantle boundary north of Tonga from the strong scattering of seismic waves. *Nature* 391: 682–685.
Vinnik LP (1981) Evaluation of the effective cross-section of scattering in the lithosphere. *Physics of the Earth and Planetary Interiors* 26: 268–284.
Wagner GS and Langston CA (1992a) A numerical investigation of scattering effects for teleseismic plane wave propagation in a heterogeneous layer over a homogeneous half-space. *Geophysical Journal International* 110: 486–500.
Wagner GS and Langston CA (1992b) Body-to-surface-wave scattered energy in teleseismic coda observed at the NORESS seismic array. *Bulletin of Seismological Society of America* 82: 2126–2138.
Wajeman N (1988) Detection of underside *P* reflections at mantle discontinuities by stacking broadband data. *Geophysical Research Letters* 15: 669–672.
Wang Y, Takenaka H, and Furumura T (2001) Modelling seismic wave propagation in a two-dimensional cylindrical whole-earth model using the pseudospectral method. *Geophysical Journal International* 145: 689–708.
Weber M and Davis JP (1990) Evidence of a laterally variable lower mantle structure from P- and S-waves. *Geophysical Journal International* 102: 231–255.
Weber M and Kornig M (1990) Lower mantle inhomogeneities inferred from PcP precursors. *Geophysical Research Letters* 17: 1993–1996.
Wegler U (2004) Diffusion of seismic waves in a thick layer: Theory and application to Vesuvius volcano. *Journal of Geophysical Research* 109. http://dx.doi.org/10.1029/2004JB003048.
Wegler U, Korn M, and Przybilla J (2006) Modeling full seismogram envelopes using radiative transfer theory with Born scattering coefficients. *Pure and Applied Geophysics* 163. http://dx.doi.org/10.1007/s00024-005-0027-5.
Wen L and Helmberger DV (1998) Ultra-low velocity zones near the core-mantle boundary from broadband PKP precursors. *Science* 279: 1701–1703.
Wennerberg L (1993) Multiple-scattering interpretations of coda-Q measurements. *Bulletin of Seismological Society of America* 83: 279–290.
Wenzel F, Sandmeier K-J, and Walde W (1987) Properties of the lower crust from modeling refraction and reflection data. *Journal of Geophysical Research* 92: 11575–11583.
Wesley JP (1965) Diffusion of seismic energy in the near range. *Journal of Geophysical Research* 70: 5099–5106.
Whitcomb JH (1973) Asymmetric PP: An alternative to PdP reflections in the uppermost mantle (0–100 km). *Bulletin of Seismological Society of America* 63: 133–143.
Whitcomb JH and Anderson DL (1970) Reflection of PP seismic waves from discontinuities in the mantle. *Journal of Geophysical Research* 75: 5713–5728.
Wright C (1972) Array studies of seismic waves arriving between P and PP in the distance range 90° to 115°. *Bulletin of Seismological Society of America* 62: 385–400.
Wright C and Muirhead KJ (1969) Longitudinal waves from the Novaya Zemlya nuclear explosion of October 27, 1966, recorded at the Warramunga seismic array. *Journal of Geophysical Research* 74: 2034–2047.
Wu R-S (1985) Multiple scattering and energy transfer of seismic waves separation of scattering effect from intrinsic attenuation I. Theoretical modelling. *Geophysical Journal of the Royal Astronomical Society* 82: 57–80.
Wu R-S (1989) The perturbation method in elastic wave scattering. *Pure and Applied Geophysics* 131: 605–637.
Wu R and Aki K (1985a) Scattering characteristics of elastic waves by an elastic heterogeneity. *Geophysics* 50: 582–595.
Wu R and Aki K (1985b) Elastic wave scattering by a random medium and the small-scale inhomogeneities in the lithosphere. *Journal of Geophysical Research* 90: 10261–10273.
Wu R-S and Aki K (1988) Multiple scattering and energy transfer of seismic waves separation of scattering effect from intrinsic attenuation II. Application of the theory to Hindu Kush region. *Pure and Applied Geophysics* 128: 49–80.
Wu W, Ni S, and Zeng X (2012) Evidence for P'P' asymmetrical scattering at near podal distances. *Geophysical Research Letters* 39. http://dx.doi.org/10.1029/2012GL052179.
Xu F, Vidale JE, and Earle PS (2003) Survey of precursors to *P'P'*: Fine structure of mantle discontinuities. *Journal of Geophysical Research* 108. http://dx.doi.org/10.1029/2001JB000817.
Yoshimoto K (2000) Monte Carlo simulation of seismogram envelopes in scattering media. *Journal of Geophysical Research* 105: 6153–6161.
Zeng Y (1991) Compact solutions for multiple scattered wave energy in the time domain. *Bulletin of Seismological Society of America* 81: 1022–1029.
Zeng Y (1993) Theory of scattered P- and S-wave energy in a random isotropic scattering medium. *Bulletin of Seismological Society of America* 83: 1264–1276.
Zeng Y, Su F, and Aki K (1991) Scattered wave energy propagation in a random isotropic scattering medium. *Journal of Geophysical Research* 96: 607–619.